DRA

(NASA-CR-159642) FEASIBILITY STUDY OF LIQUID POOL BURNING IN REDUCED GRAVITY Final Report, Jul. 1977 - Feb. 1979 (Notre Dame Univ.) 79 p HC A05/MF A01 CSCL 21B

N79-32303

Unclas G3/25 35871

Department of Aerospace and Mechanical Engineering

University of Notre Dame

Notre Dame, Indiana 46556

FEASIBILITY STUDY OF

LIQUID POOL BURNING IN REDUCED GRAVITY

by

A. Murty Kanury

FINAL REPORT OF

An Investigation Supported Under
NASA Contract NAS3-21018

NATIONAL AERONAUTICS AND SPACE ADMINISTRATION
LEWIS RESEARCH CENTER
4300 BROOKPARK ROAD
CLEVELAND, OH 44109

NASA Report CR-159642
Notre Dame TR No. 79-1

CONTENTS

Abstract

This report describes the results of a research study of the feasibility of conducting experiments in the Spacelab on the ignition of, and flame spread over, liquid fuel pools which are initially at a temperature lower than the fuel's flash point temperature. Theories are developed for the ignition and flame spread processes and experiments are conducted to understand the factors influencing the ignition process and the spread rate. The results are employed to devise a conceptual Spacelab experiment which is expected to be feasible for a safe conduct and to be suitable for obtaining crucial data on the concerned processes.

I. Introduction

The research reported here deals with the issues of feasibility of studying the burning of liquid fuel pools in reduced gravity conditions facilitated by the Spacelab. This research was sponsored by NASA under contract No. NAS3-21018 to the University of Notre Dame, Department of Aerospace and Mechanical Engineering. Based on a previous study [1] (under NASA Contract No. NAS3-20087, NASA Rept. No. CR-135234, Notre Dame TR. No. 77-33, June 1977) the specific topics of current study evolved to be ignition of, and flame spread over, fuel pools whose temperature is below the fuel's flash point.

1. Ignition: If a heated rod or a well-defined flame, or any other heat source were placed parallel to, and in the proximity of, the surface of a fuel at a temperature lower than its flash point temperature, a transient free convective flow is set-up around this source in the gas phase. This flow is strongly dependent upon gravity and establishes a thermal communication between the source and the fuel surface if the source is sufficiently close to the surface. The heat flux to and temperature of the fuel surface will be maximum directly under the source, and they will decay monotonically as one marches away from the source in a direction normal to its axis. Due to the temperature gradients along the liquid surface, surface tension gradients are set-up to produce a flow in the condensed phase. Buoyancy, shear, and inertia also come into play in this flow which forms two symmetric cylindrical cells as shown in Figure 1.

Given this situation, to determine the flow patterns, heat transfer distribution, resultant fuel vaporization, vapor dispersion in the gas phase, and ignition of the mixture constitute problems of extreme importance both in science and practice. In the present project the development of flow and heat transfer is studied to examine the influence of the properties of the fuel, fuel layer thickness, gravity, heat source strength and dimensions, etc. on the time to ignition. Experiments are discussed in Chapter V and Appendix E whereas the results of a theory presented in Appendix D are summarized in Chapter IV.

2. Flame Propagation: Once a liquid fuel is ignited as above, say at one end of a long tray, the flame would propagate over the liquid surface.

Flame propagation over a horizontal pool of fuel follows one of two possible distinct patterns [5] depending upon whether the fuel's initial temperature is above or below its flash point. When the temperature is above the flash point a combustible gas mixture exists above the liquid surface. After ignition a flame would then propagate through the combustible mixture under the control of the gas phase mechanisms of heat and mass transfer.

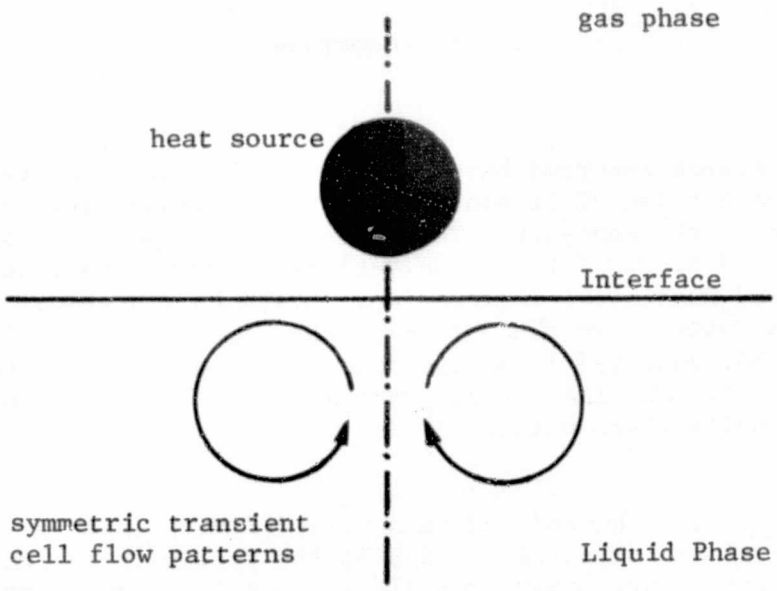

FIGURE 1: THE IGNITION PROBLEM.

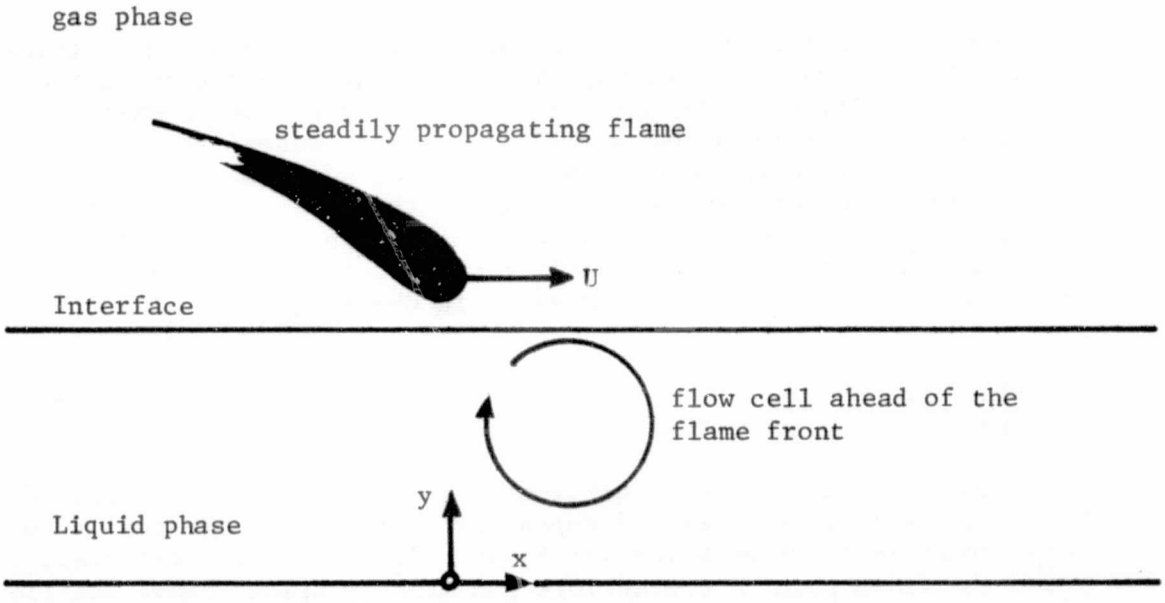

FIGURE 2: THE FLAME SPREAD PROBLEM.

When the fuel temperature is below the flash point, however, the propagating flame will have to preheat the fuel ahead of it continuously, this preheating being just adequate to raise the adjacently located fuel element to the flash point. The flame then creeps forward to this heated element and proceeds to heat the next element. Keeping aside the importance of thermal radiation, this preheating can occur by conduction and convection in both gas and liquid phases. The gas-phase heat transfer becomes inconsequential since the gas-phase conductivity is relatively negligible and since the gas-phase convective flows oppose the flame propagation direction. The liquid-phase conduction is smaller by about an order of magnitude [2] than the liquid-phase convection which occurs in the same direction as flame propagation

Experiments of Roberts [10,11], and Mackinven [6] showed that the condensed phase flow is induced by the flame itself and that the two of the most influential parameters are the liquid viscosity and the sensitivity of liquid surface-tension to the surface temperature. The liquid flow patterns set up by the combined influence of gravitation and surface tension assume the primary responsibility to transfer energy ahead of the flame front. A qualitative sketch of this flow is presented in Figure 2. Experiments on flame spread are discussed in Chapter V and Appendix E whereas the essential results of a theory developed in Appendix C are presented in Chapter III.

3. Justification: The Spacelab experimentation on liquid fuel ignition and flame propagation promises to yield valuable, otherwise unattainable, data. As discussed below, the heat and mass transfer processes leading to ignition and flame spread involve several competing or cooperative forces. Inasmuch as the total problem is much too complex, simplifications are required to be made in order to develop theories of ignition and of flame spread. These simplifications are only possible upon the knowledge of the relative importance of the various forces. This knowledge is required also to test the validity of assumptions made in theoretical studies. Earth-based experiments are unsuitable or inconvenient in attempts to isolate these forces and understand their role. Thus it is expectable that the Spacelab data are crucial in advancing the state-of-the-art of the liquid fuel combustion problem.

a. Theoretical: The unusual motions of the liquid resulting from an intricate interaction of surface-tension forces with gravitational, viscous, and inertial forces are of interest not only in science but also in practical applications. Conduct of liquid flow experiments in space gives an extra degree of variability of the gravitational constant to control the Froude number (i.e., inertial forces/gravitational forces), Bond number (i.e., gravitational forces/surface-tension forces), and no-name number (i.e., gravitational forces/viscous forces) [1]. The data obtained in the Spacelab over extended ranges of these dimensionless quantities will offer a powerful basis to verify various theoretical hypotheses on the special liquid motions.

Over and beyond aiding to satisfy one's scientific curiosity about

these motions, the Spacelab experiments are expected to lead also to a better understanding of a host of practical situations involving liquids, slurries and emulsions subjected to heating or cooling, and evaporating with or without chemical reactions. These chemical reactions may pertain to combustion or to any of the numerous chemical engineering processes.

Both ignition of liquid fuel pools and flame spread over them are expected to involve important transient effects of heat, mass and momentum transfer. These transient effects are strongly dependent on the gravitational level. At high values of g, it is also expectable that three-dimensional phenomena would overwhelm. Conduct of experiment in space where reduced gravity is possible is anticipated to enable one to delineate these and other complicating secondary aspects of the studied processes of ignition and flame spread over liquid surfaces.

Glassman's work [5-7] pointed out that surface-tension-driven flows in the liquid are of paramount importance in the convective heat transfer responsible for the flame propagation. Once again, the liquid viscosity, fuel layer depth, sensitivity of surface tension to the surface temperature are some of the critical factors in this heat transfer process.

Besides Glassman's group, Torrance [8,9] and Roberts [10,11] are among the authors who studied surface-tension flows. The available analyses are, however, unsuitable to predict the role of gravity in either aiding or opposing the surface-tension-driven flow. Conduct of experiments under low gravity conditions available in the Spacelab will permit the use of conveniently deeper pools to study the shallowness effects, for then the pools are deep enough to be instrumented or visualized but at the same time the low gravity preserves the physics by keeping low the governing Grashof, Reynolds and Marangoni numbers. (These nondimensional numbers are defined in Table I).

Torrance [8,9] computed the flame spread Reynolds number as a function of Marangoni and Grashof numbers. His main finding was that buoyancy and surface-tension work hand-in-hand to produce a thermal convection cell which enables the flame to propagate forward. The effect of buoyancy is small and nearly indistinguishable for $Gr \approx 10^4$. At Grashof number of about 10^6, buoyancy appears to influence the flows about as much as surface-tension. In contrast to this, Glassman [7] assumes gravity's influence is realized through hydrostatic pressure which opposes the surface-tension-driven flow. Under these circumstances the absence of gravity would significantly affect the flame spread rate.

It is clear that there is not a firm understanding of the role gravity plays in flame spreading processes. Carefully conducted experiments in reduced gravity offers the prospect of shedding light on these complex phenomena.

Our considerable search into the chemistry, physics and engineering literature pointed out only a few references to the ignition problem [2-4]. Dimensional and hueristic analyses point out the role played by gravity [1], but to quantify the expected results, experiments in the

TABLE I

NONDIMENSIONAL NUMBERS OF CONCERN
IN THE PRESENT STUDY

$$Gr \equiv \frac{g h_\infty^3 \rho^2}{\mu^2} \beta (T_o - T_\infty) \equiv \frac{\text{Buoyancy x Inertia}}{\text{viscous}^2}$$

$$Re \equiv \frac{\rho h_\infty U}{\mu} \equiv \frac{\text{Inertia}}{\text{Viscous}}$$

$$Ma \equiv \frac{\rho C_p h_\infty^2}{\mu K} \frac{d\sigma}{dT} \frac{dT}{dx} \equiv \frac{\text{Surface-Tension-Induced Convective Flux}}{\text{Conductive Flux}}$$

prolonged programmed gravity environment of the Spacelab are highly suitable.

Historically, the science of combustion possessed a special character in that the incubation period is relatively short for scientific concepts to become translated into important practical applications. Thus, progress made in combustion science via Spacelab experimentation may be expected to lead to prominent technological developments.

a. Experimental: If variable or low gravity experiments are thus deemed justifyable on the basis of theoretical arguments, one might question why one can not simulate the reduced gravity conditions in earth-based laboratories; and why one would require experimentation in the Spacelab. In Appendix A, a variety of currently used techniques of simulating low gravity conditions are reviewed and their various features are discussed. Some of these techniques are indeed suitable for studying some short-lived processes of fluid physics and heat transfer. However, if the process under study involves characteristic time scales of the order of minutes as do the liquid fuel ignition and flame spread, the state-of-the art simulation techniques become unsuitable, for the low-g duration offered by them amounts to the order of 10 seconds or so. Thus it appears to be eminently justified on the basis of experimental suitability to advocate liquid fuel pool experiments in the Spacelab.

b. General: Over and above these preceding analytical and experimental justifications of the study of fuel liquid ignition and flame spread in the Spacelab, there is also a more general justification. This pertains to the need to establish fire safety in the low-gravity conditions of our space vehicles in general, and in the Space Shuttle in particular. These various installations are essential and extremely expensive. Their cargo is ultra-sophisticated scientific equipment whose material value is greatly overshadowed by the value of the critical

data and information they bear to generate towards the advancement of science and solution of technological problems for mankind. Even more important is the life safety of the Spacelab personnel. Intrinsically, the options available to fight an accidental fire, or to egress to safety from it, are limited. Thus, again, it is critical to gain a thorough understanding of the processes of fire initiation and growth at low gravity conditions.

Thus it is clear that the Spacelab experiments on liquid fuel ignition and flame propagation are desirable. The theories developed in Appendices C and D and discussed in Chapter III and IV as well as the experiments described in Chapter V and Appendix E point out some further reasons why the prolonged conditions of low- or zero-gravity are desired for the study of ignition and flame spread.

II. Feasibility Issues

Once the need for further study of the liquid fuel ignition and flame spread processes is substantiated [1] and the conduct of the experiment in the essential environment provided by the Spacelab is justified analytically and experimentally, our immediate next concern is to establish the feasibility of the Spacelab experiment.

Typical questions related to feasibility examination are as follows: which particular fuels will yield the most useful results? Under what particular ranges of the independently variable conditions do these useful results arise? How safe is the conduct of the proposed experiment in the Spacelab? How large will the fuel pool have to be to give meaningful results? How would the fuel be transported, stored and loaded into the pool tray? How full would the tray be filled; is a 100% full tray possible under the influence of the curvature of surface resulting from surface-tension? How will the flow patterns be observed and recorded in both the liquid and gas phases? How are the temperature, velocity and concentration fields to be quantitatively measured in the Spacelab experiment? Are there any physical features of the ignition and flame spread processes which can be studied by observing the thermo-fluid-dynamic response of inert liquids, say water? What exactly are the hypothetical mechanisms of ignition and flame spread of liquid fuels?

The paramount issue in dealing with liquid fuels in the Spacelab appears to be that concerned with safety. It infringes upon decisions related to nearly all other design aspects of the experiments.

1. Choice of Fuels: The factors involved in this choice are: the flash point of the fuel in air; the fuel's corrosivity and toxicity; its known thermophysical properties; etc. The table of properties summarized in Appendix B leads one to believe that such fuels as benzene, xylene and toluene are undesirable because of their extreme reactivity and corrosiveness. Our experiments, described elsewhere in this report, show that alcohols are suitable, especially butanol.

2. Pool Dimensions: The fuel pan dimensions have to be small enough to alleviate a catastrophe in the event of an accidental spill and yet large enough to minimize two-dimensional effects of the side walls. Glassman's work [6] indicates that not unless a width of about 0.60 meters or more is employed will one realize a flame spread process uninfluenced by the side-walls. Since this magnitude of a width is clearly unacceptable for the Spacelab experiment, we propose to use a small width but by developing theoretically and verifying experimentally at 1-g the influence of pool width. A three-dimensional theory has to be developed to segregate clearly the effects of the pool width on the ignition and flame spread processes. Our feasibility study experiments on butanol pools ranged in width from about 2 cm to 10 cm, as reported in Appendix E of this report.

The depth of the pool has to be so chosen as to avoid impeding the surface-tension-driven flow cell whose dimension depends on various properties of the fuel and flame as discussed in Appendix C. For butanol this depth was found to be about 1 to 2 cm from our experiments.

Finally, the length of the tray has to permit observations free of the region in which the ignition transients dominate and from the region where the upstream boundary effects affect the condensed phase flow field. An overall length of 30-35 cm appears to satisfy these restraints for butanol pools.

3. Fuel Transportation, Storage and Handling: Based on the Claussius Clapeoron relation between the saturation vapor pressure and temperature, it appears that the fuel could be transported and stored in a variable pressure container. The flash point temperature is merely the temperature of the liquid at which, corresponding to the prescribed total pressure, a critical vapor pressure is developed over the liquid surface. The criticality is stipulated by the lean limit of flammability. It appears that for a given transportation and storage temperature of the liquid, the lower the maintained total pressure the higher will be the flash point relative to the storage temperature. Thus one can transport and store fuel at a low pressure safely and then introduce it into the pan at a higher pressure, the level of which is determined by the desired flash point relative to the supply temperature. This technique of transporting the fuel safely is suitable for fuels whose normal flash point is close to the ambient temperature of the experimental facility. For fuels such as butanol whose flash point is considerably higher than the supply or ambient temperature, safe transport and storage are much easier.

A method of handling the fuel in this safer situation is described in the conceptual design of Spacelab experiment. This method recognizes that the volume of liquid required per experiment in the chosen pan is about 270 mℓ. This volume corresponds to a sphere of diameter ≈ 8 cm. If a pair of hemispherical clamshells are fabricated with flanges which can be bolted together to form a spherical chamber with an elastic membrane in-between them, the required amount of fuel could be loaded on one side of this membrane. Employing compressed air, the fuel could be displaced into the pool tray or sucked back into the sphere after an experiment. The technique definitely offers a controlled and safe transportation, storage, and handling of fresh fuel and stowage of used fuel.

4. The Filling Process, Stability of the Free Surface: With the fuel transported/stored employing the spherical container discussed above, the filling process is quite simple. As the pan is filled, what are the characteristics of the free surface as to its stability? In attempts to answer this question, Labus at NASA [12] has conducted a dimensional analysis and some simple experiments. Liquid was introduced into a precisely machined stainless steel pan which was then tipped slowly until the fluid flowed out. Denoting, for convenience, the plane of the

undisturbed surface to be 'horizontal' and its normal to be 'vertical', the limiting tilt angles θ are correlated on a horizontal Bond number ($g \sin\theta\ R^2\ \rho/\sigma$) versus vertical Bond number ($g \cos\theta . R^2\ \rho/\sigma$) plane (where g is gravitation or gravitational jitter, θ is angle of tilting from horizontal, R is pan radius, ρ is liquid density and σ is surface-tension). The results of the experiments showed that in the limit of a very small vertical acceleration environment, the critical horizontal Bond number required to retain the fluid in the pan has to be less than 2 to 3. For butanol the density $\rho \approx 0.81$ g/cm^3 and the surface-tension $\sigma \approx 25$ dynes/cm. For a pool of width 2.54 cm, the half-width R = 1.27 cm. Thus if the critical horizontal Bond number of 2 to 3 observed by Labus is valid for butanol, the maximum permitted gravity and inclination to avoid spilling by width-wise 'rocking' of the pool are given by $g\sin\theta \approx 2$ to 3 times the quantity $(\sigma/\rho R^2)$; $(g\sin\theta)_{max.permitted} \approx 38.27 - 57.4$ cm/s^2. Noting that smaller values of either gravity or g-jitter and of inclination would ensure containment of the liquid in the pan, a factor of safety of 2 would result in a maximum permitted $(g\sin\theta)$ of about 19.13 to 28.7 cm/s^2. A horizontal pan thus could be subjected to a g-jitter of as much as 0.02 to 0.03 times the normal gravity of 981 cm/s^2 before causing a spill. The g-jitter values expected in the Spacelab due to extraneous disturbances are of the order 10^{-5} times the normal g. The pan width of 2.54 cm thus appears to provide safety from spillage due to g-jitter.

If the same arguments are made based on the length-wise 'rocking' of the pan of length 2R=35 cm, the maximum permitted value of $(g\sin\theta)$ to avoid spillage is about 0.10 to 0.15 cm/s^2. The maximum permissible g-jitter to avoid spillage due to length-wise disturbances is thus about 1×10^{-4} to 1.5×10^{-4} times the normal gravity of 981 cm/s^2. Thus the spillage is a couple of orders of magnitude easier to occur due to length-wise disturbances than due to width-wise disturbances. Even the more vulnerable length-wise spillage will not be a problem with a 35 cm long butanol pool if the g-jitter is $10^{-5} g_o$ or lower.

5. Methods of Flow Visualization and Measurement: The current state-of-the-art of flow, and heat and mass transfer measurement techniques are reviewed by this author in reference 13. In the Spacelab experiment, we expect to employ particle trace techniques of flow visualization. The tracer, most probably metallic particles or aluminum oxide flakes, will be premixed in the fuel container.

III. Flame Propagation Over Liquid Pools

The basic physical picture of the flame propagation over a liquid fuel layer whose temperature is below its flash point is shown in Figure 2. The pool is assumed to be infinite in extent normal to the plane of the paper, i.e., the pool width is assumed to be irrelevant. The depth of the undisturbed pool is h_∞ so that y=0 forms the rigid base of the pool and $y = h_\infty$ refers to the liquid-air interface. Suppose a flame is initiated at $x = -\infty$ and is permitted to steadily and uniformly propagate in the $+x$ direction at a speed of U. If the frame of reference $x = 0$ is fixed on the spreading flame front, one encounters a steady phenomenon in which the flame front is at rest while the fuel and gas-phase are fed backwards into the flame.

The surface temperature of the fuel layer decreases rapidly with distance upstream of the flame front; at the flame front $x = 0$ this temperature will be equal to the fuel's flash point whereas at some positive x-value the temperature will be equal to the lower supply temperature. Since the surface-tension of most liquid fuels decreases with increasing temperatures, the nonuniformity in surface temperature would result in a nonuniformity in surface-tension. Thus the effect of surface-tension gradient in the x-direction is essentially to pull the surface liquid away from the flame front. As the hot liquid is thus carried forward in the direction of flame propagation, energy is convected to continue the propagation further.

Sirignano and Glassman [7] and Torrance [8,9] carried out theoretical analysis of the flame propagation controlled by surface-tension flow. There are four forces of interest in the problem; these are: inertial, gravitational, viscous, and surface-tensional. These four forces result in three independent parameters to describe the problem. For flows driven by surface-tension, the order of magnitude of the velocity is determined by a balance between the surface-tension force and the viscous force at the surface. Thus the ratio of surface-tension force to viscous force is of the order of unity. As shown in Table I, the ratio of inertia force to viscous force is known as Reynolds number; the ratio of buoyancy to inertial force is Froude number; the product of the ratio of buoyancy to viscous force and the ratio of inertia to viscous force is known as Grashof number; and finally the ratio of heat transfer due to surface-tension-driven convection to conductive heat flux is known as Marangoni number.

Torrance [8,9] compared the flame spread Reynolds number as a function of Marangoni and Grashof numbers. His main finding was that buoyancy and surface-tension work hand-in-hand to produce a thermal convection cell which enables the flame to propagate forward. The effect of buoyancy is small and nearly indistinguishable for $Gr \simeq 10^4$. At a Grashof number of about 10^6, buoyancy appears to influence the flows about as much as surface tension. He also predicted that the surface temperature would decrease with distance ahead of the flame front in an almost linear fashion and would become uniform at larger distances. The characteristic

length for this surface temperature is independent of the liquid layer depth but is inversely proportional to the flame spread speed. In contrast to this, Sirignano [7] assumes that gravity's influence is realized through hydrostatic pressure which opposes the surface-tension-driven flow. Under these circumstances the absence of gravity would significantly affect the flame spread rate.

In Appendix C a theoretical model of the surface-tension-controlled flame spread over a liquid fuel surface is presented. Sirignano [7] developed a similar theory but by ignoring buoyancy and by focusing on the hydrodynamic part of the problem. We considered, following Birikh [47], the energy conservation equation to obtain the temperature field from which we can account for the buoyancy term in the momentum equation. Torrance [8,9] studied this problem comprehensively by employing numerical methods of solution. Even though our solution pertains only to the field ahead of the steadily propagating flame, it is of a closed-form. The essence of Appendix C for the present feasibility study is represented by the following results of nondimensional velocity and temperature fields.

$$\bar{u} = -Re + C_1 \left[\frac{Gr}{8} \left(\frac{\bar{y}^4}{3} - \frac{9}{10}\bar{y}^2 + \frac{7}{15}\bar{y} \right) + \frac{\bar{\phi}}{2}\left(\frac{3}{2}\bar{y}^2 - \bar{y} \right) \right]$$

$$\bar{T} = (1 + C_1 \bar{x})\bar{y} + \frac{PrC_1^2}{240}\left[\frac{Gr}{420}\, a(\bar{y}) + \bar{\phi}\, b(\bar{y}) \right]$$

$$a(\bar{y}) \equiv (100\,\bar{y}^7 - 567\,\bar{y}^5 + 490\,\bar{y}^4 + 99\,\bar{y}^3 - 122\,\bar{y})$$

$$b(\bar{y}) \equiv (9\,\bar{y}^5 - 10\,\bar{y}^4 - 3\,\bar{y}^3 + 4\,\bar{y})$$

where the nondimensional quantities listed in Table II are defined as below:

$\bar{u} \equiv \rho h_\infty u/\mu$	nondimensional velocity
$Re \equiv \rho h_\infty U/\mu$	flame spread
$\bar{T} \equiv (T-T_\infty)/(T_o-T_\infty)$	temperature
$Gr \equiv g h_\infty^3 \rho^2 \beta (T_o-T_\infty)/\mu^2$	Grashof number
$\bar{\Phi} \equiv \phi\,(T_o-T_\infty)\,\rho h_\infty/\mu^2$	surface-tension parameter
$Pr \equiv \mu C_p/\kappa$	Prandtl number

$$\bar{x} \equiv x/h_\infty \qquad (0 \leq \bar{x} \leq -1/C_1)$$

$$\bar{y} \equiv y/h_\infty \qquad (0 \leq \bar{y} \leq 1)$$

$$C_1 \equiv 40\ Re/3\ \left(\bar{\phi} - \frac{11}{140}\ Gr\right)$$

u is the x-directional velocity, U is the flame spread speed. h_∞ is the undisturbed fuel layer thickness. ρ is fuel density; μ is its dynamic viscosity; T_o is its flash point; β is its volumetric expansion coefficient; ϕ is the sensitivity of surface-tension σ to temperature, $\phi \equiv d\sigma/dT$, a negative quantity; Pr is the liquid's Prandtl number; K is thermal conductivity; and C_p is specific heat. g is gravitational constant and T_∞ is fuel supply temperature.

The nondimensional surface-tension parameter $\bar{\phi}$ is related to the Marangoni number mentioned earlier in a straight-forward way. To obtain the constant C_1 in the form given above constitutes the essence of the theory presented in Appendix C. For $\bar{x} > 1/C_1$, $\bar{u} = -Re$ and $\bar{T} = 0$ uniformly.

Figure 3 shows the velocity profile in the fuel layer as predicted. Inasmuch as the temperature profile is linear with respect to $\bar{x}$, this velocity profile is independent of $\bar{x}$ in the domain $0 \leq \bar{x} \leq -1/C_1$. The flow reversal is evident from Fig. 3. Additionally it can be seen that the effects of increased surface tension sensitivity and reduced gravity are cooperative. The parameter $Gr/\bar{\phi}$ in this figure is a measure of the relative intensity of gravitational and surface-tension forces. $Gr/\bar{\phi} = 0$ refers to zero-gravity situation while $Gr/\bar{\phi} = -\infty$ refers to zero-surface-tension-gradient situation. $Gr/\bar{\phi} = -60$ approximately corresponds to the situation encountered in the earth-based laboratory with a 2.5 cm thick layer of a fuel such as butanol.

Reduction or absence of gravity, in general increases the flow velocity at the surface. This increase, according to the continuity equation, is only possible at the expense of a decrease in maximum negative velocity at a $\bar{y}$ of about 1/3. Note also that the velocity gradient $\partial\bar{u}/\partial\bar{y}$ at the surface approaches zero as gravity increases towards infinity relative to the surface-tension-gradient. This is understandable, for any shear at the free surface has to be balanced by the surface-tension force. It is interesting to note that our resultant velocity profile, when $Gr/\bar{\phi}$ is set to zero, coincides with the Levich profile. And finally, the influence of reduced gravity on the velocity profile is rather abrupt; this can be seen by noticing that whereas the difference between the velocity profiles of $Gr/\bar{\phi} = 0$ and $Gr/\bar{\phi} = -60$ is considerable, the difference between the profiles of $Gr/\bar{\phi} = -60$ and $-\infty$ is relatively minor.

The temperature profiles are shown in Figure 4 (flame spread Reynolds number is 2) and 5 (Re = 10). The surface-tension parameter $\bar{\phi}$ and Prandtl number Pr are kept fixed respectively at -100 and 45 but three different Grashof numbers are considered. The temperature, of course, varies

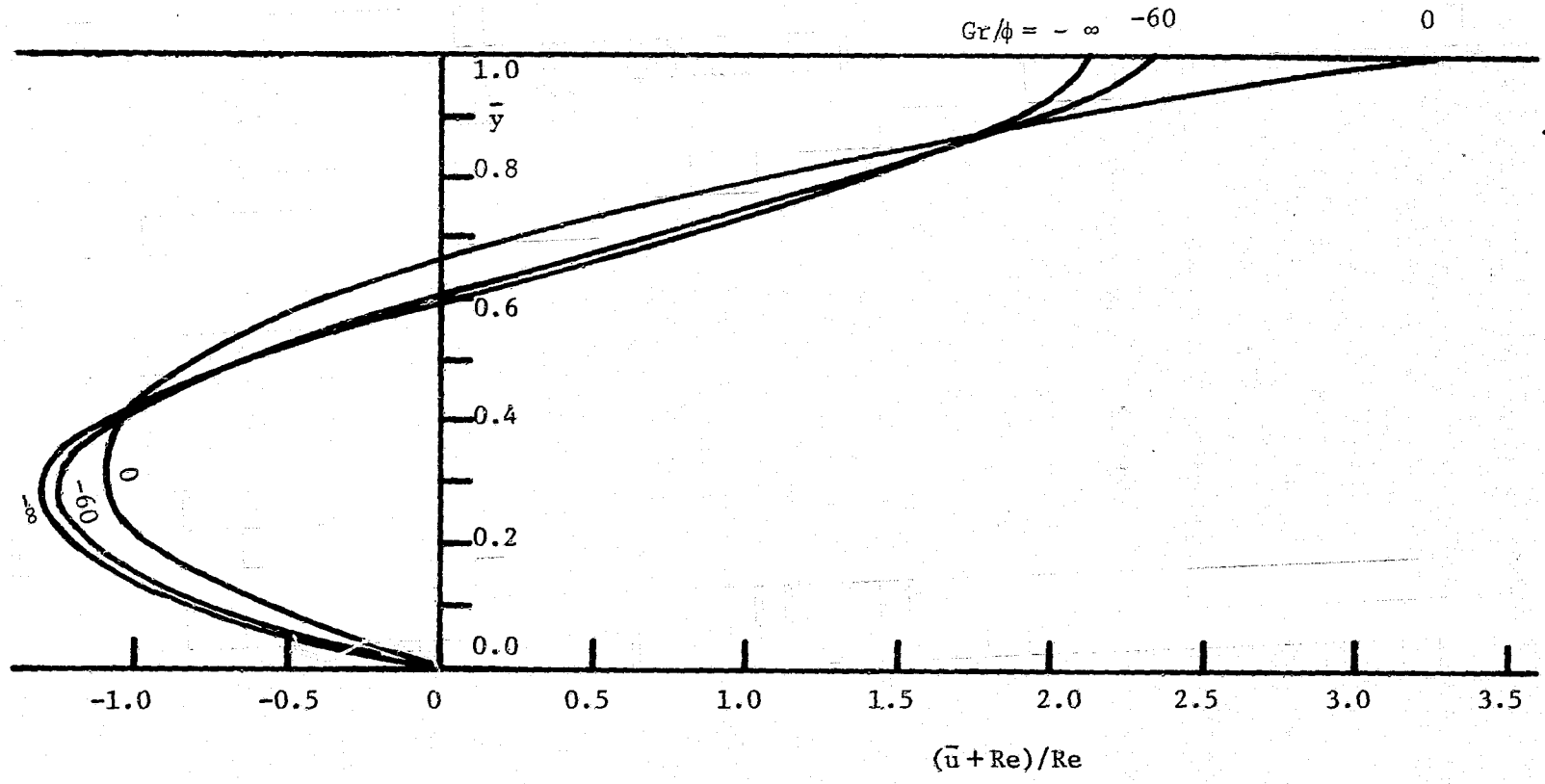

FIGURE 3: THE VELOCITY PROFILE IN THE FUEL LAYER AS INFLUENCED BY GRAVITY, SURFACE TENSION AND FLAME SPEED.

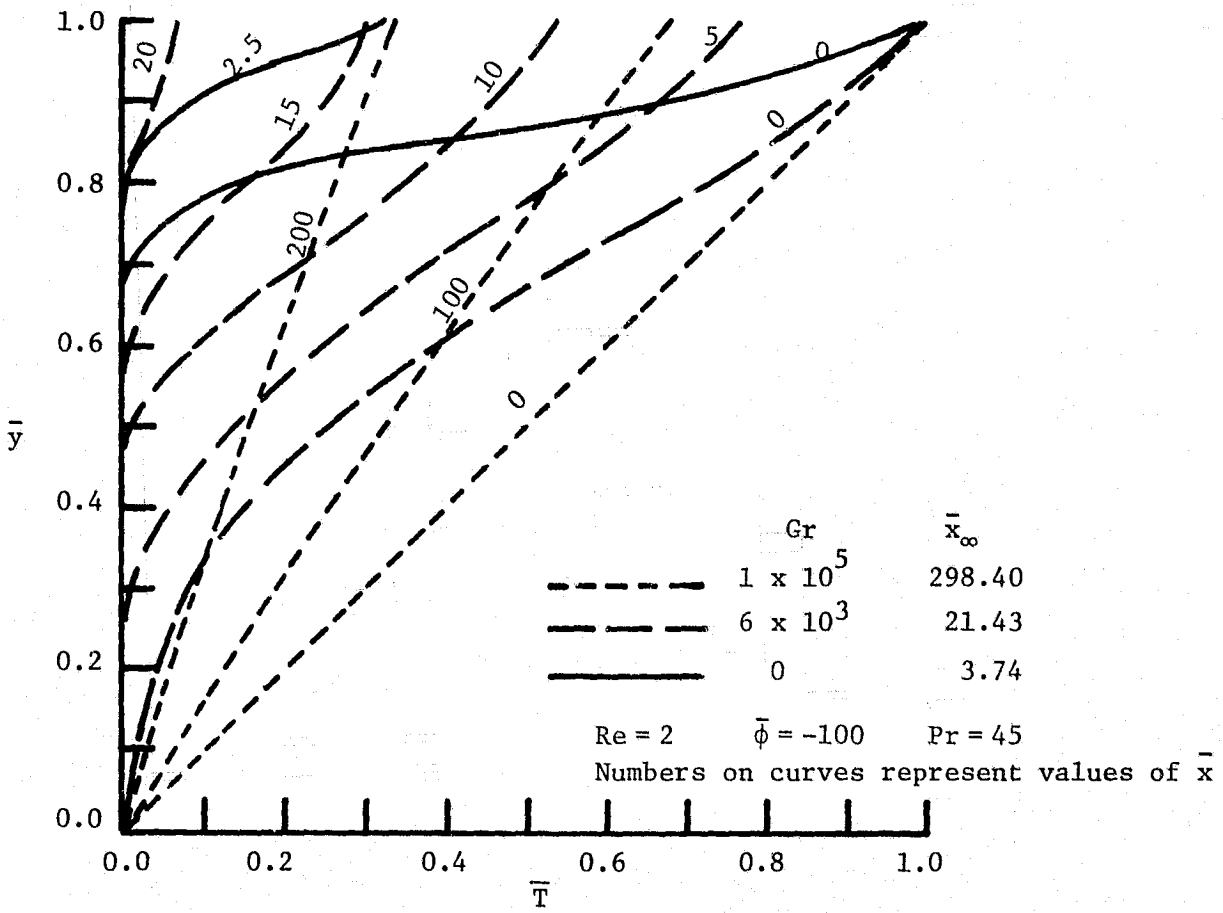

FIGURE 4: TEMPERATURE PROFILES IN THE FUEL LAYER AS INFLUENCED BY GRAVITY AT FIXED Re, $\bar{\phi}$ and Pr.

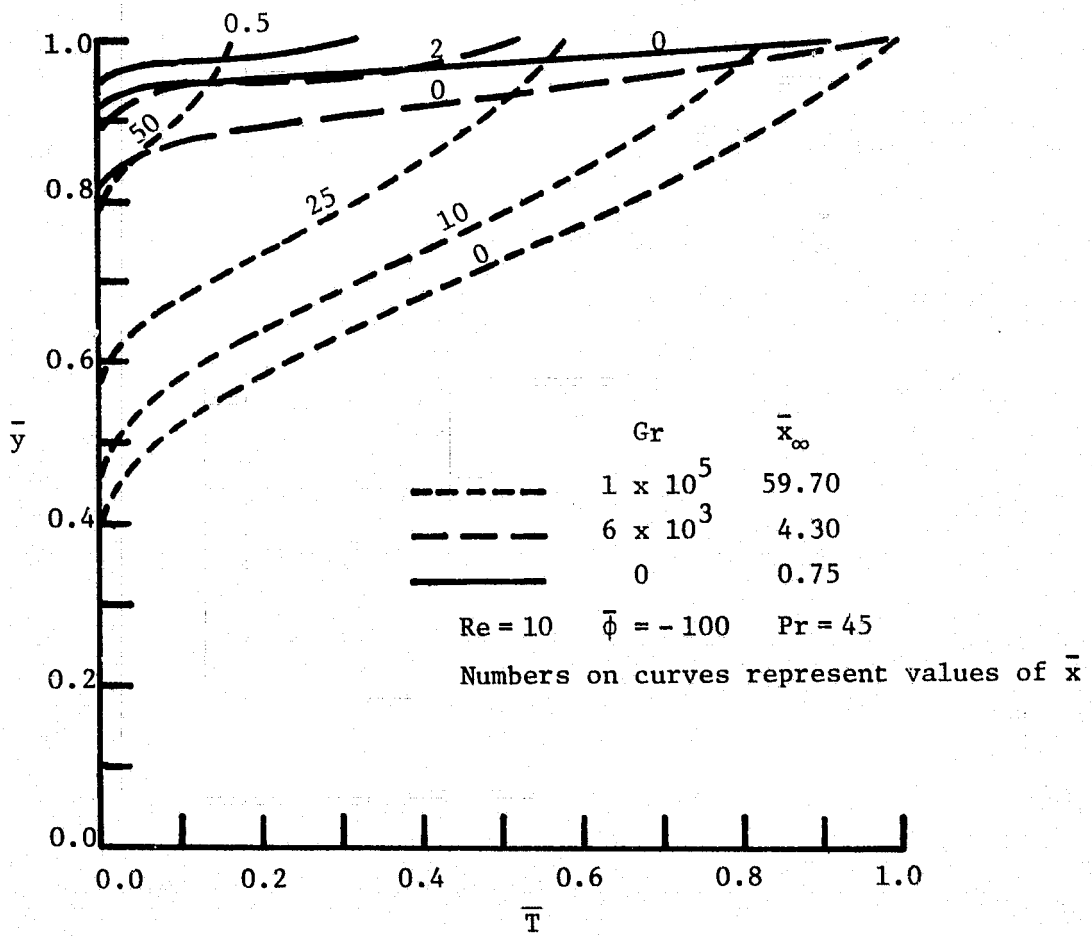

FIGURE 5: TEMPERATURE PROFILES IN THE FUEL LAYER AS INFLUENCED BY GRAVITY AT FIXED Re, $\bar{\phi}$ AND Pr.

between a maximum of unity and a minimum of zero.

It is clear that the larger the gravity the greater the penetration of the thermal disturbance into the liquid layer. It is also clear that slowly propagating flames will result in a deeper penetration of the thermal effects. Furthermore, the temperature effects reach deeper as one approaches (in $\bar{x}$-direction) the flame's leading edge.

In Figure 6 the surface temperature as a function of $\bar{x}$, distance from the flame front, is shown specifically as dependent upon the flame spread Reynolds number, surface-tension parameter and Grashof number. The linear relation is an assumption in the present theory. However simpler analyses lead to the expectation of this linearity even though one's intuition can not readily lead to it. The linearity is altogether consistent with Torrance's [8,9] numerical solutions of the full governing equations.

To find the slope of the $\bar{T}_s(\bar{x})$ linear relation constitutes the essence of the theory presented in Appendix C. This slope, denoted by C_1, is given above. Faster propagating flames, over pools of fuels with lower surface-tension parameter $\bar{\phi}$, at lower levels of gravity produce steeper decay of the surface-temperature with distance $\bar{x}$. The influence of the gravity and flame spread rate are much stronger on this steepness than the influence of surface-tension.

The slope C_1 has the importance that it indicates the extent of forward thermal influence, $\bar{x}_\infty = -1/C_1$, exerted by the combined Gr and $\bar{\phi}$ effects. It is thus useful in delineating the length required of the Spacelab pool experiment. For alcohols, $\bar{\phi} \approx -100$ to -200 and $Re \approx 1$ to 10. Earth-based experiment on pools, about 2 to 3 cm deep, of alcohol have a Gr of about 6000. Thus one can see from Figure 6 that the region of forward thermal influence is about an order of magnitude shorter in zero-g than in normal-g.

The $\bar{x}_\infty$ - dependency on Grashof and Reynolds numbers, and the surface-tension parameter is portrayed in Figures 7 and 8 in order to graphically show the involved sensitivities. We must stress again that the influence of reduced gravity appears to be to reduce the length of thermally disturbed region. Reduction in surface-tension gradients and increase in flame spread velocity also have the same consequence albeit less strong.

How do we employ these inferences in choosing the dimensions of the Spacelab experiment? The viscous forces at the base of the pool tend to elongate the recirculatory mass of the fluid. For any chosen depth, the distance ahead of the flame front to which the motion and thermal disturbances extend is of the order of ten times the depth in an earth-based laboratory whereas it is of the order of one to three times the depth at zero-gravity. Thus choosing a pool of depth 2.54 cm (arbitrarily picked for convenience) the region of length-wise interest is expected to be about 2.54 to 7.5 cm at zero-gravity. For suitable observations, therefore, a 15-20 cm observation length of the pool is deemed adequate with about 7-15 cm ignition transient length and about 7.5 cm length for

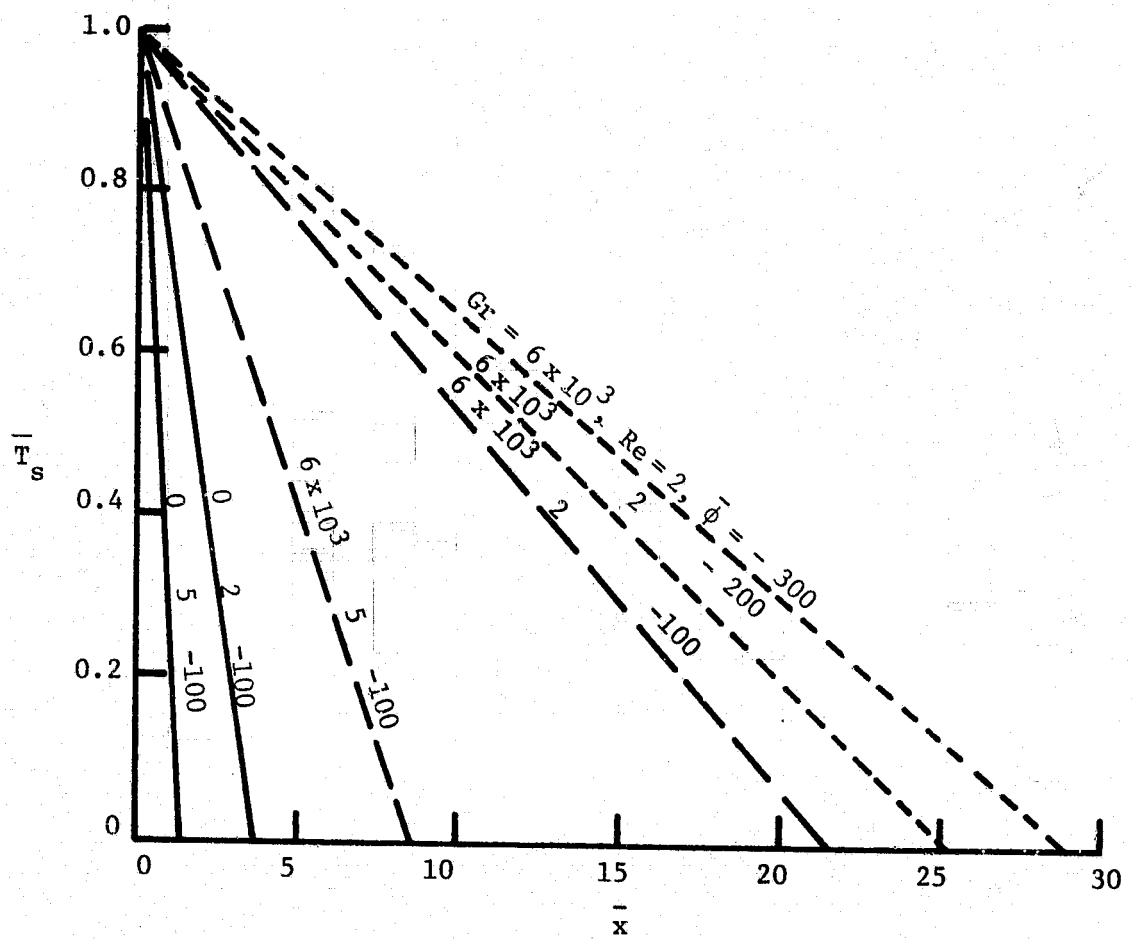

FIGURE 6: SURFACE TEMPERATURE VARIATION AHEAD OF THE SPREADING FLAME.

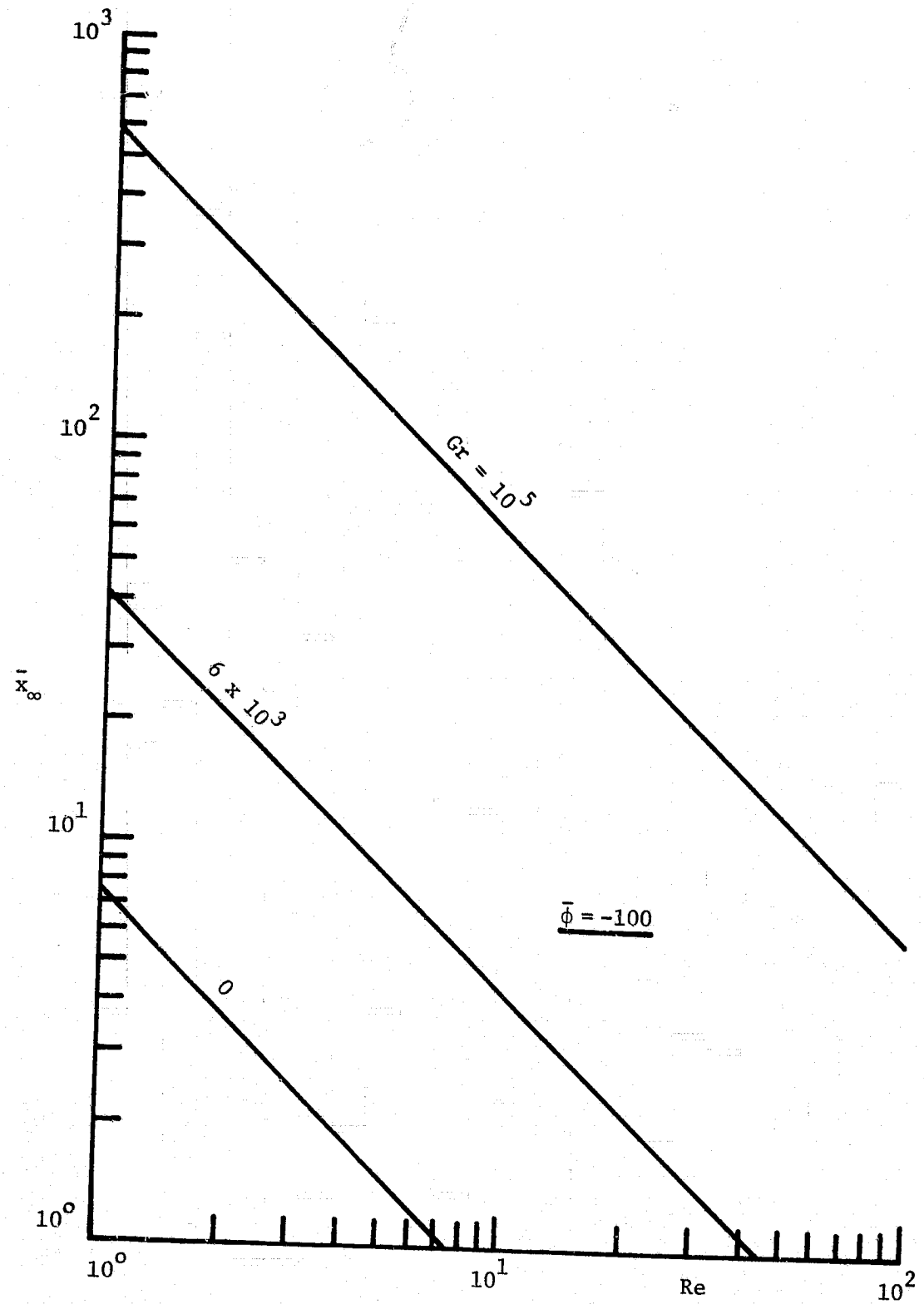

FIGURE 7: FORWARD REGION OF DISTURBANCE AS DEPENDENT ON GRAVITY AND FLAME SPREAD RATE AT $\bar{\phi} = -100$.

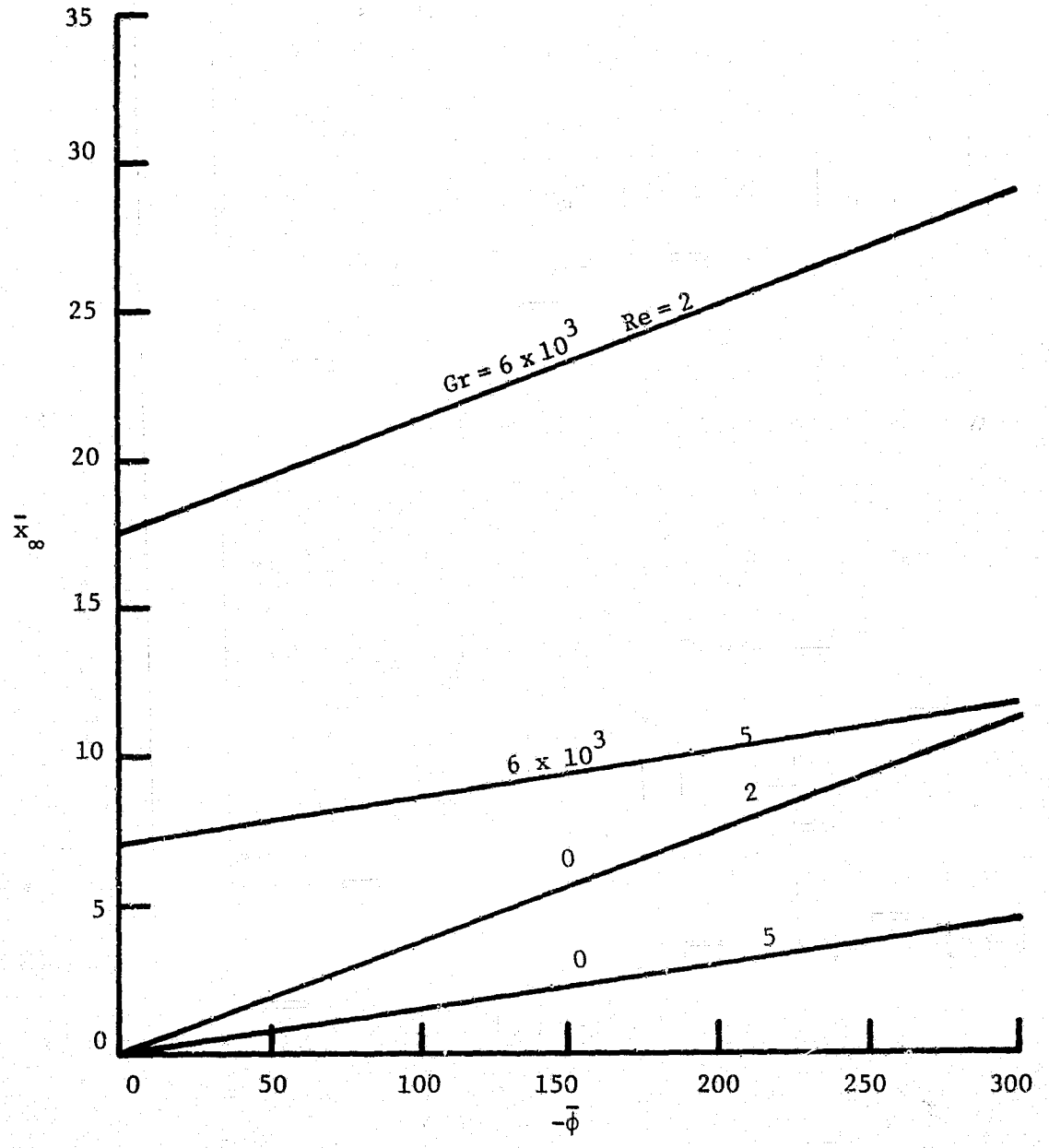

FIGURE 8: FORWARD REGION OF DISTURBANCE AS DEPENDENT ON GRAVITY, SURFACE TENSION PARAMETER AND FLAME SPREAD RATE.

alleviating the suppression effects of the upstream boundary. Ignition transient length is the distance from the ignition point in which the flame would induce itself to a state of steady propagation. From the analysis of the ignition problem presented in Appendix D and summarized in Chapter IV and from the experiments discussed in Chapter V and in Appendix E, this length is expected to be about 7-15 cm in zero-gravity and about 10-15 cm at normal gravity.

The Spacelab pool, according to these considerations, is to be about 30-40 cm long, 2.54 cm deep and an arbitrary width of 2.54 cm.

IV. Ignition

As a quiescent fuel layer of thickness h_∞ is subjected to a heat source of strength $\dot{q}'$ watts per unit length in the pool-width direction, heat transfer occurs to the liquid transiently, surface-tension-driven flow would ensue along with natural convection and there would arise an instant at which the liquid is locally raised to its flash point to result in ignition. A mathematical model is presented for this problem in Appendix D. The main results of this theory pertain to the transient development of the extent of flow and thermal perturbation, the surface velocity and the liquid temperature averaged over the region of disturbance. The following results are obtained.

Disturbance size:

$$\bar{\Delta} = \left(\frac{\bar{d}\left(\frac{Gr}{20} - \bar{\phi}\right)\bar{q}}{2} \right)^{1/5} \left(\frac{15\,\bar{t}}{4\pi} \right)^{2/5}$$

Surface velocity:

$$\bar{u}_s = \frac{1}{4} \left(\frac{\bar{q}\left(\frac{Gr}{20} - \bar{\phi}\right)}{2\,\bar{d}\,(\bar{\Delta}-\bar{x})} \right)^{1/2}$$

Liquid temperature at surface:

$$\bar{T}_s = \left(\frac{2\,\bar{q}\,(\bar{\Delta}-\bar{x})}{\bar{d}\left(\frac{Gr}{20} - \bar{\phi}\right)} \right)^{1/2}$$

$\bar{d}$ is the diameter of ignition source, $\bar{\phi}$ is surface-tension sensitivity to temperature, Gr is Grashof number and $\bar{q}$ is power fed to the ignitor, all dimensionless as defined below along with the nondimensional time $\bar{t}$, dimension of disturbance $\bar{\Delta}$ and velocity $\bar{u}$.

$$\bar{x} \equiv x/h_\infty \quad ; \quad \bar{d} \equiv d/h_\infty \quad ; \quad \bar{\Delta} \equiv \Delta/h_\infty$$

$$\bar{u}_s \equiv \rho h_\infty u_s/\mu \quad ; \quad \bar{t} \equiv \mu t/\rho h_\infty^2 \quad ;$$

$$\bar{\phi} \equiv \phi(T_o - T_\infty)\,\rho h_\infty/\mu^2 \quad ; \quad \bar{q} \equiv 4f\dot{q}'/\mu\, C_p(T_o - T_\infty);$$

$$Gr \equiv g h_\infty^3 \rho^2 \beta\,(T_o - T_\infty)/\mu^2.$$

x is distance along the liquid surface; d' is essentially the diameter of the ignition source; h_∞ is the pool depth, Δ is cell dimension;

PAGE 22 INTENTIONALLY BLANK

u_s is surface velocity; ρ is liquid density; μ is dynamic viscosity; t is time; ϕ is $d\sigma/dT$, σ being surface-tension; T_o is fuel flash point temperature; T_∞ is fuel supply temperature; $\dot{q}'$ is power input to the ignitor per unit length in the direction of the pool's width; f is fraction of $\dot{q}'$ delivered to the pool; C_p is heat capacity of the liquid; g is gravitational acceleration, and β is the volumetric expansion coefficient of the liquid. It is interesting that the dimension of the disturbance would grow with time raised to the power 2/5. The greater the Grashof number and $-\bar{\phi}$, the larger the growth. A heat source large in size and strength would also enhance the growth. If $\bar{\phi} = -100$, the $\bar{\Delta}$ at the same heating rate and time at zero-g will be about 75% of its value at the earth's gravity (i.e., $Gr \approx 6000$). If $\bar{\phi} = -200$, this fraction becomes about 83%. This somewhat unexpectedly weak influence of gravity makes the earth-based studies of preignition flow patterns useful in interpreting the results of the Spacelab experimental data.

Note from the surface velocity equation given above that at time near zero, $\bar{\Delta}$ being small, an impulsive motion is set up in the liquid surface. This prediction is consistent with the findings of MacDonald [4].

As the transient build-up of motion and heating continues, ignition of the liquid is said to have occurred at the instant when the surface temperature at $\bar{x} = 0$ reaches the flash point. Thus setting $\bar{T}_s = 1$ at $\bar{x} = 0$ in the solution, the ignition conditions (denoted by asterisk) are obtained.

$$\bar{t}^* = \frac{\pi \bar{d}^2 \left(\frac{Gr}{20} - \bar{\phi}\right)^2}{15\, \bar{q}^3}$$

$$\bar{\Delta}^* = \frac{\bar{d}\left(\frac{Gr}{20} - \bar{\phi}\right)}{2\bar{q}}$$

$$\bar{u}^*_{s_{\bar{x}=0}} = \frac{1}{4}\frac{\bar{q}}{\bar{d}}$$

For alcohols $\bar{\phi} \approx -100$ to -200. If $\dot{q}'$ lies between 0.1 and 1.0 kW/m, $\bar{q} \approx 1.5 - 15$ with alcohol supplied at about 300 ^oK. The heat wire diameter can be ranged such that $\bar{d}$ lies between 0.05 and 0.20. The gravity and surface-tension effects conspire together to determine the ignition time and the extent of the disturbed region as shown in Figure 9.

The ignition time and extent of disturbed fluid are larger with a thicker ignitor, keeping all else fixed. The surface velocity at this time directly under the heater, however, will be lower with thicker ignitor. Furthermore, the ignition time is inversely proportional to the cube of heating rate. This strong dependency arises because the fluid velocity itself is a linearly increasing function of $\bar{q}$; the resultant enhancement in the convective dissipation of energy is the reason why it

takes much longer to arrive at the ignition condition.

Note from Fig. 9 that ignition time as well as the flow region dimension are significantly reduced by reducing gravity to zero. For example, with a $\bar{q}$ of 15 and $\bar{d}$ of 0.20, $\bar{t}^* = 0.4$ in an earth-based laboratory and 0.025 in the Spacelab; the corresponding values of $\bar{\Delta}^*$ are respectively 2.6 and 0.67. At other values of $\bar{q}$ and $\bar{d}$ similar differences exist between the earth-based laboratory and the Spacelab as listed below:

$\bar{q}$	$\bar{d}$	$\bar{t}^*$ earth	$\bar{t}^*$ Spacelab	$\bar{\Delta}^*$ earth	$\bar{\Delta}^*$ Spacelab
1.5	0.04	16	1	5.4	1.3
1.5	0.20	400	25	26	6.5
15	0.04	0.016	0.001	0.54	0.13
15	0.20	0.4	0.025	2.6	0.65

From this table, one can see that under expectable heater and fuel layer circumstances, a maximum, $\bar{\Delta}^*$ of about 6 is realized in a reduced gravity environment. Thus, if our Spacelab pool is arbitrarily chosen to be 2.54 cm deep, for convenience, the preignition disturbance will extend as far as 0.33 cm to 15 cm. The ignition time t^* is expected to lie in the range 0.125 sec. to several minutes.

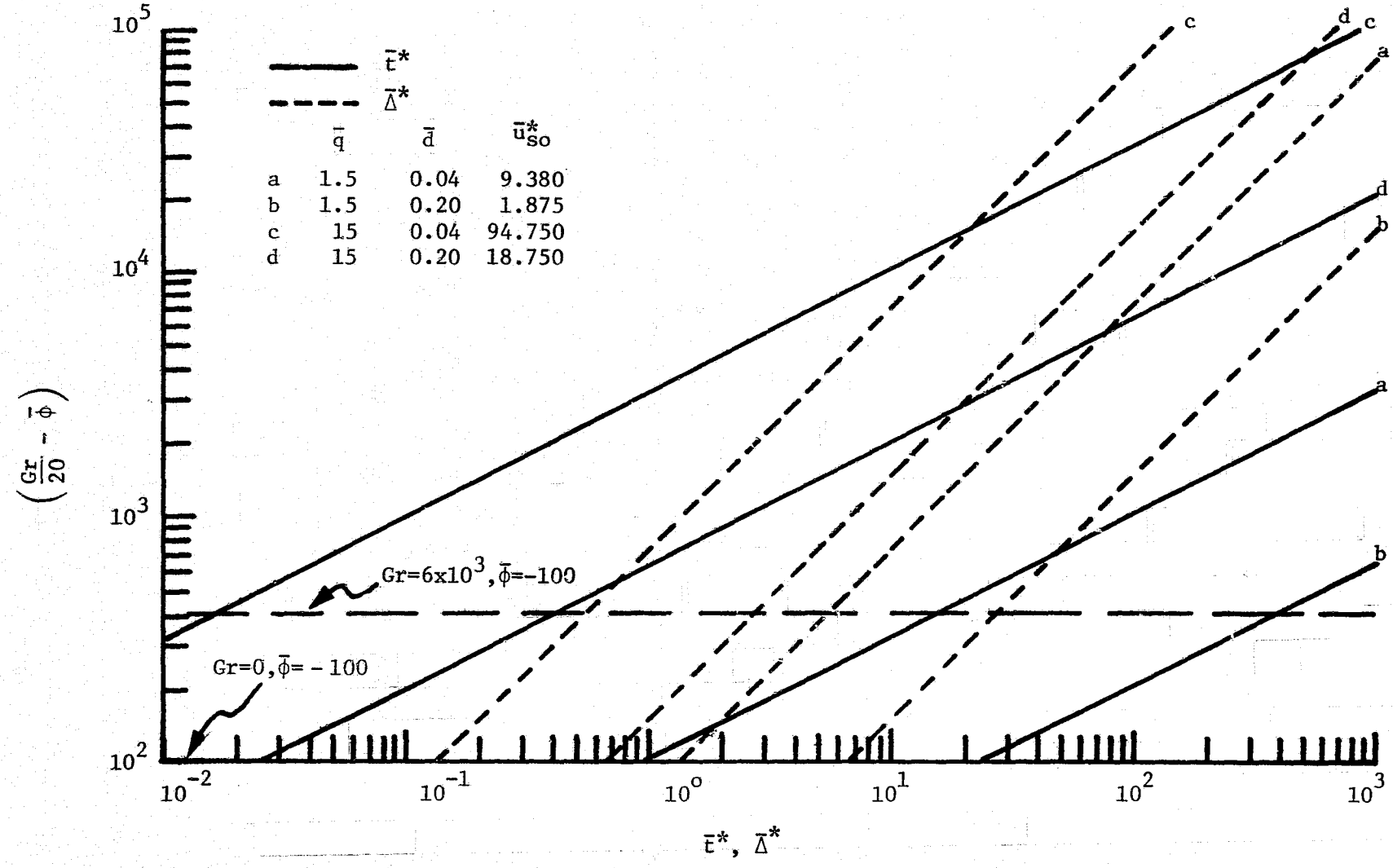

FIGURE 9: TIME TO IGNITION AND THE THEN EXTENT OF DISTURBANCE AS DEPENDENT ON GRASHOF NUMBER, SURFACE TENSION PARAMETER, HEAT SOURCE SIZE AND STRENGTH.

V. Experimental

The experimental part of this project, described in detail in Appendix E, led to the following conclusions of relevance in the feasibility issues.

(a) A tray of dimensions 2.54 cm wide, 2.54 cm deep and about 35 cm long appears to be suitable to obtain meaningful data on preignition and flame spread. The depth is chosen arbitrarily for convenience in handling the fuel. The width effects appear to be amenable for isolation by a 3-d theoretical study and earth-based experiments.

(b) Disturbances in the fluid during the preignition heating appear to extend to about 10 cm.

(c) The steadily propagating flame on 2.54 cm deep butanol appears to produce flow and thermal perturbations to a distance of about 10-15 cm ahead of the flame front. This distance is in reasonable agreement with the flame spread theory. In zero-gravity environment, the theory leads us to expect that this distance will be much smaller, i.e., about 1.5 - 7.5 cm.

(d) The tray could be fabricated out of an aluminum frame with inserted plateglass sidewalls.

(e) The environmental temperature and humidity appear to be of little consequence on the observed flame spread rate. The room drafts, however, are expected to disturb the propagating flame.

(f) The nature of fuel effects the flame spread-related and ignition-related processes drastically. Whereas the flash point temperature at the operational air pressure is the most important property of the fuel, the liquid-air interfacial tension and its sensitivity to temperature are also crucial. Other properties of concern include the liquid density, specific heat, thermal conductivity, viscosity, etc.

(g) Xylene, a ring compound is found in our experiments to be extremely corrosive.

(h) Commercial kerosene, a usually poorly defined mixture of several hydrocarbons, is quite suitable for preignition and flame spread experiments, but the data can not be employed to test theoretical hypothesis because of the unknown physico-chemical properties.

(i) Butanol is found to be a well-defined and suitable fuel for further work. The only minor drawback of this fuel is its ability to absorb and dissolve water vapor from the flames.

(j) The flame spread rates are erratically large as the initial supply temperature of the fuel approaches its flash point. The most

orderly observation of the butanol flame spread process in 1 atm air can be done at temperatures below about 38°C.

(k) The free-board height is to be chosen either to be zero (i.e., the fuel surface is flush with the top edge of the tray walls) or to be larger than 6 mm (i.e., the fuel surface is over 6 mm below the top edge of the tray walls).

(l) Flame spread rate is larger in trays of larger widths. The side wall effects appear to be greater at larger fuel supply temperatures. A tray width of 2.54 cm appears to be suitable for the Spacelab experiments. The observed flame spread rates and flow patterns could then be corrected for the width-effects.

(m) There appears to be a linear relationship between the flame spread rate and the pool depth. The slope is larger for larger fuel supply temperature. For pool depths greater than about 1.5 cm the linearity is well-established.

(n) The flame spread rate may be influenced by the ignitor disturbances to an extent of about 10-15 cm on the ignitor end. However, the effect of the upstream end-wall (on the opposite end) may be felt by the flame for about 10-15 cm also. A length of 15 cm in the middle of a 35 cm long tray is deemed long enough to obtain data on a flame whose spread rate is uninfluenced by the end effects.

(o) Butanol fuel exhibits quite vivid liquid flow patterns when exposed to a small propane flame (about 5 mm in diameter and 1.5 cm in length) placed at a distance of about 5 mm above the surface. Observation of the transient development of the surface-tension-driven convection flow is possible and the ignition time is of the order of 0.1 to 1 sec.

(p) Surface-tension-driven flow is not observed in water layers subjected to a propane flame exposure. Even though one would expect these flows theoretically, the inevitable contaminants of water precludes them in practice.

VI. Conceptual Design of the Spacelab Experiment

Description of the Experiment: The objectives of pool burning experiments in the Spacelab are to make: (i) qualitative observations; (i) quantitative testing of various gravity-related hypotheses; and (iii) quantitative examination of the various assumptions made in theoretical studies. The experiments have to be such as to be uniquely possible only in the essential environment of the Space. Both the qualitative and quantitative studies will relate to flame spread and ignition aspects of pools of fuels at temperature lower than their flash point. These studies must lead to a distinct advance in the state-of-the-art and science of combustion of liquid fuels.

Whereas the quantitative data are expected to enable us to verify the expected or speculated phenomena, the qualitative observations will serve two specific purposes. First, they aid to consolidate the quantitative measurements in some detail, say via photographic visualization. Second, they will reveal some features, phenomena, and processes which have not been identified before in our project research.

The experiments would also establish the thresholds of validity of various concepts and notions, and existence of different limiting modes of flame spread and ignition. This would in effect lead to identification of limiting combinations of conditions which would permit a particular phenomenon to occur. Not only new useful information but also novel unfamiliar notions are expected to evolve out of these threshold delineations.

The experiment to be carried out in the Spacelab must fulfill certain inherent constraints. The experimental set-up has to be large enough to permit the planned observations and measurements, and yet small enough to (a) permit visualization through limited-view-angle photographic means and (b) assure safety of the Spacelab and its crew in the event of a spill. The set-up has to be relatively insensitive to extraneous disturbances (such as g-jitter). It should require little or no calibrational effort in flight; and must be as much automated as possible to avoid potential human error.

Figure 10 shows a schematic of the conceptual Spacelab experiment. The heart of this experiment is the pan which holds the fuel. This tray is expected to be made of Pyrex. The dimensions of this pan are 2.54 cm wide, 2.54 cm deep and 35 cm long. The false bottom, whose height location can be adjusted by two thumb screw posts, is provided so that the test depth of the fuel layer can be adjusted to any value between about a few millimeters to about 2.54 cm. The idea of an adjustable false bottom is conceptually quite attractive; but in practice it may be much easier to replace pans of different depths.

In the back of the tray, a ruler scale marked in mm divisions is attached. Sliding horizontally under the ruler is a shutter, made of a fireproof material such as asbestos, which when in position will snuggly

1. Pyrex tray (2.54 x 2.54 x 35 cm)
2. False Bottom
3. Ruler Scale
4. Shutter Extinguisher
5. Gas Phase Thermocouple
6. Ignition Spark Rod
7. Accelerant Pipette

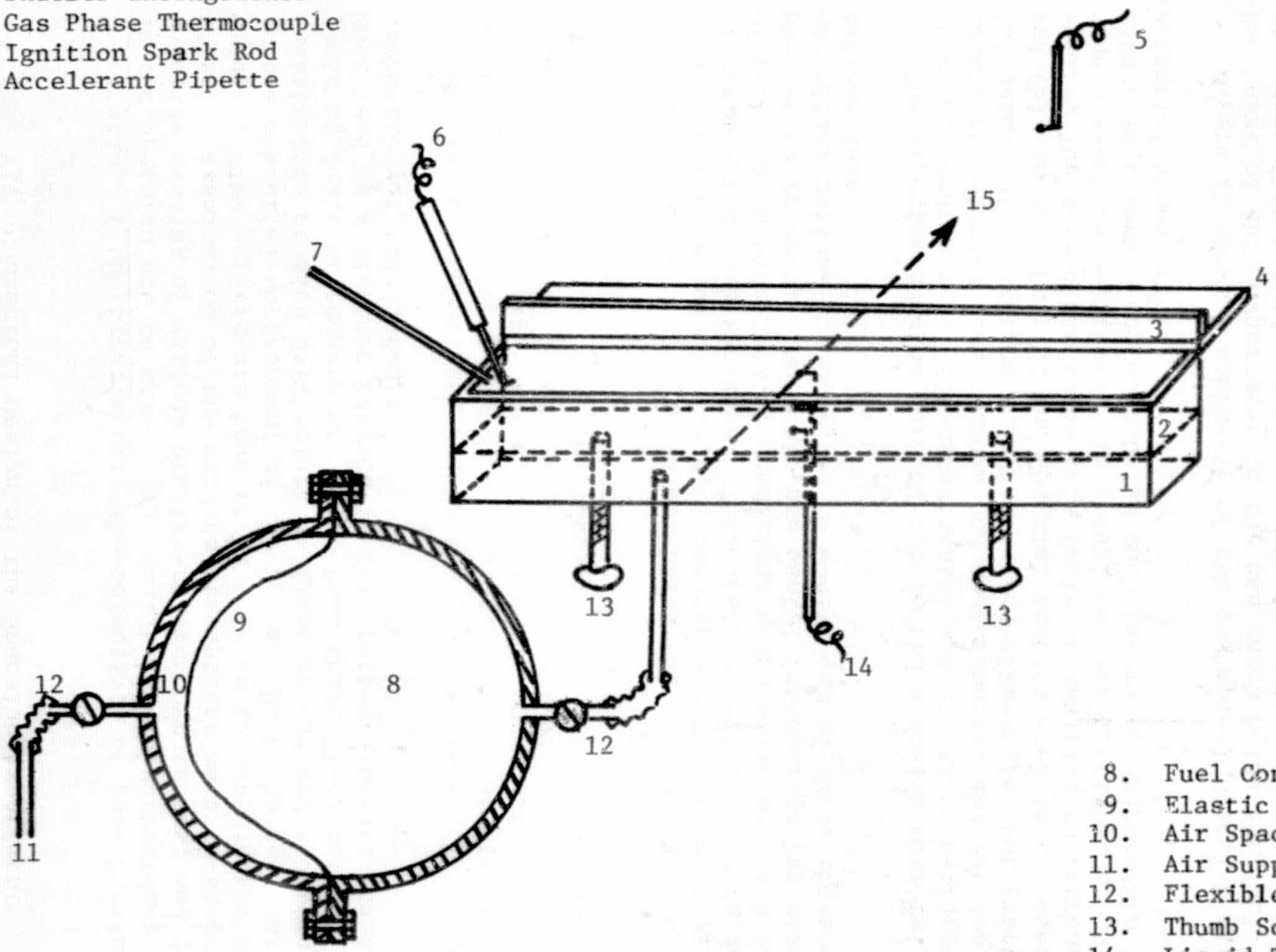

8. Fuel Container (≈ 8 cm dia.)
9. Elastic Membrane
10. Air Space
11. Air Supply
12. Flexible Connections
13. Thumb Screws
14. Liquid Thermocouple Outputs

FIGURE 10: CONCEPTUAL DESIGN.

cover the 2.54 cm wide, 35 cm long tray. Upon completion of an experiment, this shutter is mechanically slid forward to extinguish the flame.

Supply fuel is introduced into the tray through a port at the bottom. The false bottom will be so dimensioned as to loosely fit in the 2.54 x 3.54 cm tray such that the fuel introduced under it will slowly fill the entire tray to the desired free-board (of zero or over 6 mm) height. This scheme is expected to produce the least disturbances in the pool during the fuel-loading process. The fuel itself will be carried aboard the Lab in containers (perhaps spherical) of inside diameter ≈ 8 cm. This would provide enough volume (≈ 270 ml) of fuel to fill the tray 100% full. The containers have to be provided with an internal elastic membrane - introduction of compressed air to one side of which would expel the fuel on its other side into the fuel tray. Upon completion of the test, the used fuel can be drawn back into the container by permitting leakage of the air. Perhaps a well-designed cylindrical syringe is an alternative to this spherical shell concept. On one end of the tray, a pipette will be arranged in such a way as to gently deliver a few drops of an accelerant (such as methanol) whose flash point is low enough to be ignited by an electrical spark. The accelerant has to possess, additionally, a high dynamic viscosity to preclude rapid spreading over the test fuel surface. It also should be immiscible in the test fuel.

About midway along the length of the pool, three fine wire thermocouples will be placed in the liquid, one at the surface, one at mid-depth and the third at the false bottom. A single thermocouple will also be used to continuously monitor the test chamber gas phase temperature before, during, and after the flame spread test.

A flow tracer, perhaps finely ground particles of magnesia or alumina will be predispensed into the fuel supply container which can be shaken thoroughly before expelling the fuel into the tray. Besides the thermocouple outputs, the majority of data of flow patterns in the liquid and gas phases and the flame spread itself are expected to be obtained on 'film' or 'tape' via high speed photography.

As far as study of preignition motion is concerned, an electrically heated rod of a known diameter is expected to be used as heat source. Its longitudinal location will be at the midpoint of the tray. The separation distance between the fuel surface and the ignitor is adjustable. Motion picture records will yield both the time to ignition and the flow patterns preceding this event.

Procedure: The following major steps constitute the procedure of the flame spread experiment.

1. Place the tray in the chamber.
2. Adjust the false bottom to the desired depth.
3. Install the thermocouple rake in the tray, and the gas phase thermocouple.
4. Connect the fuel container to the tray.

5. Connect air supply to the container.
6. Actuate the shutter to check its operation. Deactuate.
7. Position the ignition rod and accelerant pipette in place. Actuate spark to check.
8. Agitate the fuel container to mix the flow tracers.
9. Admit air to fuel container to slowly introduce the fuel into tray to the rim.
10. Turn on the thermocouple data acquisition system.
11. Note the initial temperature of fuel, and chamber pressure and temperature.
12. Turn the camera on.
13. Note the settling of the fluid disturbances.
14. At time-2, introduce accelerant.
15. At time 0, strike the ignition spark.
16. Observe and record.
17. As the flame spreads all along the tray, activate the shutter extinguisher.
18. Turn off the data acquisition systems and cameras.
19. Release air from the fuel container to retrieve the spent fuel.
20. Disconnect the container from the tray and the air supply from the container.
21. Mark and stow away the spent fuel container.
22. Vent the chamber.
23. Go to step 2 above.

The preignition study experiment involves similar steps as follows:

1-6. Same as above.
7. Position the ignition source at the midlength in the middle of the tray rim.
8-13. Same as above.
14. Initiate energy flow to the ignitor.
15. Set time = 0.
16. Observe and record.
17. When ignition occurs activate the shutter extinguisher.
18-23. Same as above.

APPENDIX A

Simulation Techniques

There are five bench-testing methods useful to simulate gravitational effects. These are to: (i) use bodies of progressively smaller physical dimension [14-18]; (ii) use other extraneously applied and controllable body forces; (iii) use a centrifuge upon the arm of which the experiment is allowed, or made, to slide; (iv) use variable pressure in the fluid to alter gas-phase density [19-22]; and (v) use dyes in a water tank, the dyes being chosen variously buoyant relative to the working fluid, namely the water [23-25].

These bench methods of simulation share some common concepts. Because gravity-dependent forces usually appear in our considerations in the form $\rho g d^3$ of the density or density differentials, gravitational constant and the linear dimension cubed, it is conceivable to control in an experiment the relative intensity of these forces by adjusting one or more of these variables. It is also possible to adjust gravity forces relative to other forces by suitably manipulating the magnitude of these 'other forces'.

For example, the gravitational force may be reduced relative to the capillary force by reducing the Bond number $Bo = \rho g d^2/\sigma$. This may be done by reducing ρ, gravity g or dimension d or by increasing the surface-tension σ [15]. Porous wicks and sponges to hold liquids in any desired geometrical form illustrate the role of small pore size d which is in essence same as that of a reduced gravity constant g. Similarly, gravitational forces may be reduced relative to inertial force by increasing the Froude number $Fr = \rho V^2/\rho g d$ which may be done not only by reducing g and/or d but also by increasing the velocity V. A reduction in the Grashof number $Gr = g d^3 \rho^2 \beta \Delta T/\mu^2$, as an additional example, reduces the gravity force relative to inertial and viscous forces. This reduction again may be accomplished equally well by reducing gravity g, or by reducing the density ρ [19-21] and the linear dimension d [15].

There are, however, practical constraints in employing indirect methods of simulating low-g conditions. Among these constraints in employing indirect methods of simulating low-g conditions are the following:

(1) Probing Difficulties: It is obvious that increasing difficulty is encountered in placing various measurement devices in an experiment as the scale of the experiment gets progressively smaller. The disturbances caused by the presence of the probes and their supports also become progressively and unacceptably severe.

(2) Physical and Chemical Limitations: As the density is progressively reduced to bring about the same effects as brought by the reduced gravity, certain physical and chemical limitations are approached. Examples of the physical limitations may be seen by considering the role

played by pressure as a basic thermodynamic property of the working fluid and as an essential factor in the definition of a continuum fluid. Examples of chemical limitations may be identified by considering the role played by pressure in determining the reaction kinetics and mechanisms, no matter whether they are simple or complex.

Heat transfer mechanisms, which are relevant not only to maintain combustion but also to suppress combustion, also suffer with the intrusion of slip-flow effects (Knudsen free molecule flow effects) as the gases become rarified and non-continuum. If reduced gravity conditions were sought to be obtained by reducing the density differentials, a whole set of novel heat transfer problems are encountered in the limit of vanishing driving potentials. These novel problems pertain to systems only slightly perturbed from their equilibrium states.

(3) Short Life-Times: An examination of the time scales of interest in thermal response of the condensed-phase, vaporization, diffusion and mixing in gas-phase and combustion of fuels indicates that small-scale experiments last far too briefly to permit the required measurements. The availability of suitable measuring tools with acceptable precision and accuracy as well as fast response is a matter of separate but related concern.

Consider the condensed-phase hydrostatics and dynamics, for an example. Suppose one wishes to employ Bond-number modeling. Then to preserve the Bond number $\rho d^2 g/\sigma$ invariant with a particular liquid, $d^2 g$ is to be kept invariant i.e., $d \propto g^{-1/2}$. If the Bond number considered is much greater than unity, that is in gravity-dominant regime, with Froude number $\sim$ 1 the characteristic time $t \propto (d/g)^{1/2}$ which with the Bond number model becomes $t \propto d^{3/2}$. Similarly, if Bo is much smaller than unity and Reynolds number is of the order of unity, that is in capillary-dominant domain, $t \propto (\rho d^3/\sigma)^{1/2}$ which for a particular liquid reduces to $t \propto d^{3/2}$ again. Clearly this 3/2-power relation is valid for all Bond numbers. Then, a reduction of length scale by a factor of (1/10) reflects in a characteristic time reduction by a factor of $(1/10)^{3/2}$ or about (1/30). This reduction can pose formidable measurement, accuracy and response problems.

Similarly, where the gas-phase convective processes are attempted to be modeled by preserving Grashof number $gd^3 \beta \Delta T \rho^2/\mu^2$, $g \propto d^{-3}$ and the response time is of the order $t \propto \mu/(\rho g d \beta \Delta T)$ so that $t \propto 1/gd \propto d^2$. A 1/10th reduction in the scale of the experiment then cuts the time scale by a factor of $(1/10)^2$, that is by 1/100th. By considering modeling of other aspects, in a similar manner, the headaches associated with reduction in the linear scale of the experiment to simulate reduced gravity may be clearly seen through the more drastically reduced characteristic time.

(4) Visual Observations: Visual and photographic observations, likewise, also become immensely difficult or impossible due to the necessity of minute dimensions to be viewed in brief time frames. Speed and resolution, two often conflicting parameters of photography, are not always available to record an experiment.

Other simulation techniques employed include (a) conducting the experiment in a freely falling chamber with various counterweights to achieve different g-levels; and (b) conducting the experiment in an aircraft whose flight trajectories are so prescribed as to realize the desired g-variation.

Free-fall simulation of low-g has been reported in the literature quite extensively. The two most noteworthy groups working in this area are from Japan [26-28] and US NASA-Lewis Research Center [29-34]. The time available in a free-fall facility is of the order $t \sim h^{0.5}/2.2$ sec, h being the height of fall in meters. A height of 5 meters thus gives about one second of fall time. In order to double this time, the height has to be increased to about 20 meters; and to triple it, nearly 45 meters. The air resistance to the falling capsule becomes a severe problem with large fall heights. A double-capsule system, in which the outer capsule acts as a drag shield, is employed to overcome this problem. Another technique used is to drop the capsule in a near vacuum as is done in the Lewis' 500 foot facility.

Whereas a free-fall gives an essentially zero gravity (i.e., gravity of the order 10^{-7} g), counterweights may be employed to attain various fractional gravities (i.e., g lying between $10^{-2} - 10^{0}$ g_o). One of the most important things to remember in free-fall experiments is that the characteristic time of the phenomenon under study has to be less than the fall time. This requirement is not always met, especially in experiments dealing with liquid fuel evaporation, vapor/air mixing and combustion. Furthermore, transiting the experimental conditions from 1-g to 0-g, the disturbances are not quickly dissipated. As a result, the true initial conditions of the zero-g experiment are not well defined. Thus the finite and short duration of the low gravity ends up to be one of the mortal shortcomings of the free-fall technique.

Aircraft executing Keplerian flight trajectories are used to obtain longer durations of low and programmed gravity conditions. Kimzey [35-39] used this technique to study combustion of various polymers. Free-floating capsules are normally used to isolate the experiment from the air frame. The practical aspects of flying the airplane pose time limitations which permit only about 10 seconds of true zero-g for experimentation. Maneuvering the aircraft in such a manner as to avoid collisions between the experiment capsule and the airplane walls is not the easiest of the tasks for the pilot even if one is satisfied with this short true zero-g duration.

APPENDIX B

SOME RELEVANT PROPERTIES OF SOME LIQUID FUELS

	Fuel	Formula	Mol. wt	ρ g/cm^3	Δh_c kcal/g	Δh_v cal/g	C_{Pl} cal/g°C	C_{Pv}	lean limit % vol.	BP@latm °C	FP	IGN Spont. °C	Viscosity Cp(@ °C)	Surf. Tension dyne/cm (@ °C)
1.	Methanol	CH_3OH	32	0.800	4.74	263	0.57	0.40	5.5	64.5	15.5	470	0.82(0) 0.60(20) 0.46(40) 0.40(50)	24.5(0) 22.6(20)
2.	Ethanol	C_2H_5OH	46	0.790	6.40	200	0.56	0.46	3.5	78.5	21.7	392	1.77(0) 1.20(20) 0.83(40) 0.59(60) 0.50(70)	24.1(0) 23.0(10)* 22.75(20)* 21.90(30)*
3.	Acetone	$(CH_3)_2CO$	58	0.791	7.36	125	0.51	0.34	2.1	56.2	- 9.4	538	0.40(0) 0.32(25) 0.28(41)	26.21(0) 23.70(20) 21.16(40)
4.	n-Hexanol	$(CH_3)(CH_2)_5OH$	102	0.814	8.70*	-	-	-	-	158	74	-	-	-
5.	n-Butanol	$(CH_3)(CH_2)_3OH$	74	0.810	8.60*	-	-	-	1.45	117.5	43.3	343	5.2(0) 3.4(15) 2.3(30) 1.4(50) 0.93(70)	26.2(0) 24.6(20) 22.1(50)
6.	Pentanol	$(CH_3)(CH_2)_4OH$	88	0.811	-	-	-	-	-	137.3	40.5	343	-	-
7.	n-Decane	$(CH_3)_2(CH_2)_8$	142	0.730	10.56	86	0.52	0.40*	0.70	174.1	43.9§	208	0.92(20)	-
8.	n-Nonane	$(CH_3)_2(CH_2)_7$	128	0.718	-	-	-	-	0.74	151	31.1§	206	0.71(20)	-
9.	n-Dodecane	$(CH_3)_2(CH_2)_{10}$	170	0.749	-	-	-	-	0.60	216	74§	204	1.35(25)	-
10.	Dipentene	$C_{10}H_{16}$	136	0.840	-	-	-	-	-	178	68.3	-	-	-
11.	o-xylene	C_8H_{10}	106	0.897	10.30	80	0.41	0.40*	1.0	144	23.9	464	1.1(0) 0.88(16) 0.81(20) 0.63(40)	30.1(0)
12.	Kerosene	--	--	0.81*	10.30*	70	0.46*	0.40*	0.6	250*	49§	260*	-	-
13.	2-n-Octanol	$(CH_3)_2(CH_2)_5CHOH$	130	0.822	9.70	-	-	-	-	86	82.2	-	10.6(15)	27.53(20)
14.	Benzaldehyde	C_6H_5CHO	106	1.042	7.92	-	-	-	1.4	178	73.9	192	1.39(25)	40.04(20)
15.	Benzyl alcohol	$C_6H_5CH_3O$	108	1.042	10.16*	84	0.38	0.40*	1.3*	205	104.4	436	5.8(20)	27.7(10)* 28.5(20)* 27.4(30)*

Source: various handbooks
* our estimate
§ closed cup

APPENDIX C

Flame Spread Theory

Consider a fuel layer of undisturbed depth h_∞ at an initial temperature T_∞ situated in a chamber of pressure P_a. Let this fuel's flash point be T_o, density ρ, dynamic viscosity μ, surface tension (with ambient air) σ, thermal diffusivity α, and Prandtl number Pr (Figure 11).

Suppose a flame is initiated over this liquid surface at $x = -\infty$ and allowed to steadily propagate at a velocity U in the positive x-direction. We will measure y from the fixed bottom surface of the pool y=0, to the free surface y=h. x=0 is fixed on the steadily propagating flame. The fuel layer is of infinite width in z-direction. The x- and y-directional velocity components are u and v respectively, as shown in Fig. 11. In the chosen coordinate system, the flame front remains stationary while the fuel layer is fed backwards into the flame at a steady velocity. As a result of nonuniform surface temperature distribution near x=0, surface-tension gradients are invoked to cause perturbation of the flow from the uniform -U flow.

The objective of our study is to obtain the flow and thermal fields in the fuel layer as dependent upon the various properties mentioned above, especially the flame spread velocity, surface-tension gradient, gravitational constant and flash point.

In the following, we employ Boussineq approximation, i.e., density of the liquid is constant in all respects except in producing buoyancy. The steady state continuity equation is written as

$$\frac{\partial u}{\partial x} + \frac{\partial v}{\partial y} = 0$$

Integrating from y = 0 to h, where h is the fuel depth,

$$\int_0^h \frac{\partial u}{\partial x}\, dy + v_s(x) - v_o = 0$$

Since the base is impervious $v_o = 0$ so that

$$\int_0^h \frac{\partial u}{\partial x}\, dy + v_s(x) = 0 \qquad (1)$$

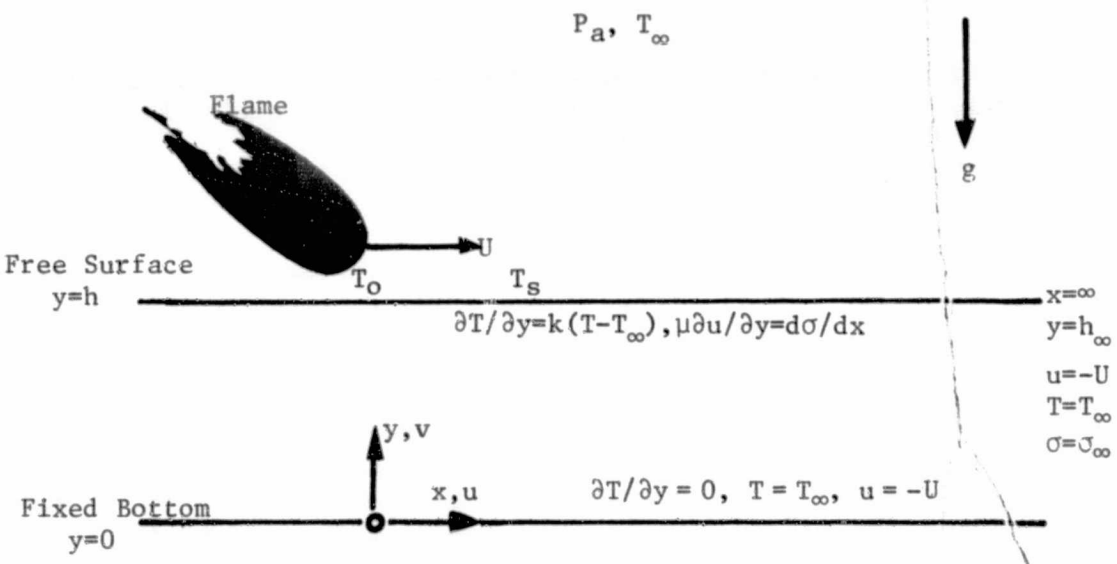

FIGURE 11: FLAME SPREAD SCHEMATIC

The Leibnitz rule says

$$\int_{a(\beta)}^{b(\beta)} \frac{\partial f}{\partial \beta}\, d\gamma = \frac{\partial}{\partial \beta} \int_{a}^{b} f(\gamma,\beta)d\gamma - f(b,\beta)\, \frac{db}{d\beta} + f(a,\beta)\, \frac{da}{d\beta}$$

so that Eq. (1) becomes

$$\frac{\partial}{\partial x} \int_{o}^{h} udy - u_s \frac{dh}{dx} + u_o \frac{dh_o}{dx} + v_s = 0 \qquad (2)$$

The third term is identically zero since the base is rigid. We denote the x-component velocity at the free surface u(h) by u_s. Now the velocity in the y-direction at the free surface is composed of two parts: first, due to displacements in the free surface which under steady state becomes $u_s dh/dx$ by geometrical considerations and second, due to surface evaporation v_{se}. Neglecting evaporation, Eq. (2) becomes

$$\frac{d}{dx} \int_{o}^{h} udy = 0 \qquad (3)$$

Equation (3) is valid irrespective of the variance (or constancy) of h with respect to x. Integrating Eq. (3), and applying the boundary condition that far ahead of the flame the velocity is uniform and equal to -U.

$$\int_{o}^{h} udy = - Uh_{\infty} \qquad (4a)$$

That is, the velocity distribution u(y) at any x will be such that the mass flow rate is independent of x. The momentum and energy equations are:

$$u \frac{\partial u}{\partial x} + v \frac{\partial u}{\partial y} + \frac{1}{\rho} \frac{\partial P}{\partial x} = \frac{\mu}{\rho} \nabla^2 u \qquad (5a)$$

$$u \frac{\partial v}{\partial x} + v \frac{\partial v}{\partial y} + \frac{1}{\rho} \frac{\partial P}{\partial y} = \frac{\mu}{\rho} \nabla^2 v - g + g\beta(T-T_{\infty}) \qquad (6a)$$

$$u \frac{\partial T}{\partial x} + v \frac{\partial T}{\partial y} = \alpha \nabla^2 T \qquad (7a)$$

All properties are considered invariant. Viscous dissipation of energy is ignored. ∇^2 is the Laplacian operator. P is pressure, μ is dynamic viscosity of the liquid and α is its thermal diffusivity. In the following paragraphs arguments are presented to further simplify these

conservation equations.

It will be assumed that the axial diffusion of vorticity and heat are both negligible. This requires that terms of the form $\partial^2/\partial x^2$ be neglected. In addition inertia terms in the momentum equations and convection of heat normal to the surface in the energy equation will both be neglected. Equation (5) thus becomes

$$\frac{\partial P}{\partial x} = \mu \frac{\partial^2 u}{\partial y^2} \tag{5b}$$

As the y-directional velocity component v and its derivatives are negligibly small, Eq. (6a) reduces to

$$\frac{\partial P}{\partial y} = - \rho g + \rho g \beta (T - T_\infty) \tag{6b}$$

and Eq. (7a) to

$$u \frac{\partial T}{\partial x} = \alpha \frac{\partial^2 T}{\partial y^2} \tag{7b}$$

Equations (5b) - (7b) have to be solved along with Eq. (4a) in the domain $0 \leq y \leq h$, $0 \leq x < \infty$ under the following boundary conditions.

At the base, $y = 0$, since no slip is permitted, $u = -U$. We will assume that the base is a perfectly conducting boundary kept at a temperature T_∞ (which is also the temperature of both the supply fuel and the atmospheric air).

At the free surface $y = h$ the pressure is assumed to be uniform and equal to the atmospheric pressure P_a. The shear in the x-direction at the free surface has to be balanced by the surface-tensional stress, $\mu \partial u/\partial y = d\sigma/dx$, σ being the surface tension of the liquid-atmospheric air interface. Furthermore, at $y = h$, we assume that the temperature gradient $\partial T/\partial y$ is proportional to the difference between the local temperature T and the ambient temperature T_∞.

Also at the free surface but at $x = 0$, the temperature of the fuel is equal to the flash point T_o. Written mathematically these boundary conditions are as follows:

$y = 0$	$u = - U$	all x	(8a)
$y = 0$	$T = T_\infty$	all x	(9a)
$y = h$	$\mu \partial u/\partial y = d\sigma/dx$	all x	(10a)
$y = h$	$\partial T/\partial y = k(T - T_\infty)$	all x	(11a)
$y = h$	$T = T_o$	$x = 0$	(12a)
$y = h$	$P = P_a$	all x	(13a)

All y	$u = -U$	$x \to \infty$	
All y	$T = T_\infty$	$x \to \infty$	(14a)

The velocity u is nondimensionalized as $\bar{u} \equiv \rho h_\infty u/\mu$. The flame spread velocity $\bar{U}$ is specially denoted as $Re \equiv \rho h_\infty U/\mu$. The temperature is reckoned relative to the fuel's initial temperature T_∞ and normalized by the difference between the flash point T_o and initial temperature, T_∞ so that $\bar{T} \equiv (T-T_\infty)/(T_o-T_\infty)$. x and y are measured in units of the pool depth so that $\bar{x} \equiv x/h_\infty$ and $\bar{y} \equiv y/h_\infty$. The pressure is rendered nondimensional according to $\bar{P} \equiv \rho h_\infty^2 P/\mu$. When one substitutes these nondimensional variables into the governing equations, the problem at hand reduces to the following:

$$\frac{\partial \bar{P}}{\partial \bar{x}} = \frac{\partial^2 \bar{u}}{\partial \bar{y}^2} \tag{5}$$

$$\frac{\partial \bar{P}}{\partial \bar{y}} = Gr\left(-\frac{1}{\beta \Delta T} + \bar{T}\right) \tag{6}$$

$$\frac{\partial^2 \bar{T}}{\partial \bar{y}^2} = Pr\ \bar{u}\ \frac{\partial \bar{T}}{\partial \bar{x}} \tag{7}$$

$$\int_o^{\bar{h}} \bar{u} d\bar{y} = -Re \tag{4}$$

$\bar{y} = 0$	$\bar{u} = -Re$	all $\bar{x}$	(8)
$\bar{y} = 0$	$\bar{T} = 0$	all $\bar{x}$	(9)
$\bar{y} = 1$	$\partial \bar{u}/\partial \bar{y} = \bar{\phi}\partial \bar{T}/\partial \bar{x}$	all $\bar{x}$	(10)
$\bar{y} = 1$	$\partial \bar{T}/\partial \bar{y} = \bar{k}\bar{T}$	all $\bar{x}$	(11)
$\bar{y} = 1$	$\bar{T} = 1$	$\bar{x} = 0$	(12)
$\bar{y} = 1$	$\bar{P} = \bar{P}_a$	all $\bar{x}$	(13)
all $\bar{y}$	$\bar{u} = -Re$	$\bar{x} \to \infty$	(14)
all $\bar{y}$	$\bar{T} = 0$	$x \to \infty$	

In the above, several dimensionless parameters have evolved. These are defined in Table II. Specifically, Gr is Grashof number, the parameter which deals with the gravitational acceleration. β is the liquid's specific volumetric expansion coefficient ($1/^{o}K$) which when multiplied by $\Delta T \equiv (T_o - T_\infty)\ ^{o}K$ becomes $\beta\Delta T$, nondimensional, a parameter specifying the expansion characteristics of the liquid. Pr is the liquid's Prandtl number, ratio of kinematic viscosity (μ/ρ) to thermal diffusivity $\alpha(\equiv K/\rho C_p)$, Re is the flame spread Reynolds number. $\bar{\phi}$ is the nondimensional sensitivity of the surface-tension σ to temperature T; $\sigma \equiv d\sigma/dt$, is assumed to be a given constant negative number; $\bar{\phi} \equiv d\bar{\sigma}/d\bar{T}$, $\bar{\sigma}$ being nondimensional surface-tension. $\bar{k}$ is simply (kh_∞) where k is the proportionality constant in Eq. (11a). Finally $\bar{P}_a$ is the nondimensional pressure of the atmosphere.

It is clear from the nondimensional version of the problem statement that the dependent variables $\bar{u}$, $\bar{T}$, and $\bar{P}$ are functions of $\bar{x}$ and $\bar{y}$ with Gr, $\bar{\phi}$, Re, Pr, $\beta\Delta T$, $\bar{k}$ and $\bar{P}_a$ as parameters. $\bar{h}$, we stress again, is a function of $\bar{x}$ which we will here assume to be a constant. This is a highly questionable assumption, the seriousness of which can only be revealed by experimental data from the Spacelab. In Table II $\bar{h} = 1$, i.e., $h = h_\infty$ according to this assumption.

Differentiating Eq. (6) with respect to $\bar{x}$ and Eq. (5) with respect to $\bar{y}$, pressure can be eliminated.

$$\frac{\partial^3 \bar{u}}{\partial \bar{y}^3} = Gr\ \frac{\partial \bar{T}}{\partial \bar{x}} \tag{15}$$

Equations (7) and (15) thus are the two equations for the two unknowns $\bar{u}$ and $\bar{T}$. Suppose now that $\bar{T}$ is a linear function of $\bar{x}$, an approximation which would imply that $\bar{u}$ is predominantly a function of $\bar{y}$ with its dependence on $\bar{x}$ being exhibited only through the constant $\partial\bar{T}/\partial\bar{x}$ at the free surface. If

$$\frac{\partial \bar{T}}{\partial \bar{x}} = C_o(\bar{y}), \tag{16}$$

substitution in Eq. (15) gives

$$\frac{\partial^3 \bar{u}}{\partial \bar{y}^3} = Gr\ C_o(\bar{y}). \tag{17}$$

This means that the left hand side is a function only of $\bar{y}$. The lower derivatives of $\bar{u}(\bar{y})$ as well as $\bar{u}$ itself are also assumed to depend on $\bar{x}$ similarly. Differentiating Eq. (7) with respect to $\bar{x}$,

$$\frac{\partial}{\partial \bar{x}} \frac{\partial^2 \bar{T}}{\partial \bar{y}^2} = Pr \left(\bar{u}\ \frac{\partial^2 \bar{T}}{\partial \bar{x}^2} + \frac{\partial \bar{T}}{\partial \bar{x}} \frac{\partial \bar{u}}{\partial \bar{x}} \right)$$

TABLE II

DEFINITIONS OF NONDIMENSIONAL QUANTITIES

$\bar{u} \equiv \rho h_\infty u/\mu$ $\qquad$ $\bar{v} \equiv \rho h_\infty v/\mu$

$Re \equiv \rho h_\infty U/\mu$ $\qquad$ $\bar{g} \equiv g h_\infty^3 \rho^2/\mu^2$

$\bar{\sigma} \equiv \rho h_\infty \sigma/\mu^2$ $\qquad$ $Pr \equiv \mu/\rho\alpha$

$\bar{P} \equiv \rho h_\infty^2 P/\mu^2$ $\qquad$ $\bar{P}_a \equiv \rho h_\infty^2 P_a/\mu^2$

$\bar{T} \equiv (T-T_\infty)/(T_o-T_\infty)$ $\qquad$ $\bar{h} \equiv h/h_\infty$

$\bar{y} \equiv y/h_\infty$ $\qquad$ $\bar{x} \equiv x/h_\infty$

$\bar{\Phi} \equiv \Phi(T_o-T_\infty)\ \rho h_\infty/\mu^2 \equiv \phi(T_o-T_\infty)h_\infty/\mu\alpha\ Pr$

$\bar{k} \equiv k h_\infty$ $\qquad$ $Gr \equiv g h_\infty^3\ \rho^2\beta(T_o-T_\infty)/\mu^2$

$\bar{d} \equiv d'/h_\infty$ $\qquad$ $\bar{\Delta} \equiv \Delta/h_\infty$

$\bar{q} \equiv \dot{q}' f4/\mu C_p(T_o-T_\infty)$

$\bar{t} \equiv \mu t/\rho h_\infty^2$

Due to the preceding assumptions related to the linearity of $\bar{T}(\bar{x})$, all terms in this equation except the first term, are zero. Hence

$$\frac{\partial^2}{\partial \bar{y}^2} \frac{\partial \bar{T}}{\partial \bar{x}} = 0$$

Integration with respect to $\bar{y}$ twice thus gives $C_o(\bar{y})$.

$$C_o(\bar{y}) = C_1 \bar{y} + C_2 \tag{18}$$

where C_1 and C_2 are integration constants. At the bottom of the pool, $\bar{T}$ is uniformly equal to zero for all $\bar{x}$. Thus Eq. (9) requires that $\partial \bar{T}/\partial \bar{x}$ be zero at $\bar{y} = 0$, so that $C_2 = 0$.

$$C_o(\bar{y}) = C_1 \bar{y} \tag{19}$$

Substituting Eq. (19) in Eq. (17) and integrating three times, we obtain the velocity.

$$\bar{u} = Gr\ C_1 \frac{\bar{y}^4}{4!} + C_3 \frac{\bar{y}^2}{2!} + C_4 \bar{y} + C_5 \tag{20}$$

C_3, C_4 and C_5 are integration constants, constants as C_1 is a constant to the extent $\partial \bar{T}/\partial \bar{x}$ is independent of $\bar{x}$.

Integrating Eq. (19) with respect to $\bar{x}$,

$$\bar{T} = C_1 \bar{y}\ \bar{x} + f(\bar{y}) \tag{21}$$

where $f(\bar{y})$ is a function to be determined from Eq. (4). Substituting Eqs. (19) and (21) in Eq. (7),

$$\frac{d^2 f}{d\bar{y}^2} = Pr\ C_1\ \bar{u}\,\bar{y}$$

which can be integrated wth $\bar{u}(\bar{y})$ known from Eq. (20). The result with Eq. (21) gives $\bar{T}$.

$$\bar{T} = Pr\ C_1 \left[5GrC_1 \frac{\bar{y}^7}{7!} + 3C_3 \frac{\bar{y}^5}{5!} + 2C_4 \frac{\bar{y}^4}{4!} + C_5 \frac{\bar{y}^3}{3!} \right] + (C_6 + C_1 \bar{x})\,\bar{y} + C_7 \tag{22}$$

The six constants $C_1, C_3, \ldots C_7$ are now to be obtained from Eqs. (4), (8)-(12). Of special interest is that if Eq. (11) has to hold for all $\bar{x}$, $\bar{k}$ is required to be unity. (This would correspond to a unit Biot number situation in thermal conduction.)

$$C_1 = \frac{40\ \mathrm{Re}}{3\left(\bar{\phi} - \frac{11}{140}\ \mathrm{Gr}\right)}$$

$$C_3 = \frac{3}{2}\left(\bar{\Phi} - \frac{3}{20}\ \mathrm{Gr}\right) C_1$$

$$C_4 = \frac{1}{2}\left(\frac{7}{60}\ \mathrm{Gr} - \bar{\Phi}\right) C_1$$

$$C_5 = -\ \mathrm{Re}$$

$$C_6 = 1 + \frac{\mathrm{Pr\ Re}\ C_1}{6} - \frac{\mathrm{Pr}\ C_1^{\,2}}{240}\left(\frac{23}{420}\ \mathrm{Gr} - \bar{\Phi}\right)$$

$$C_7 = 0$$

Applying these constants to Eqs. (20) and (22) and sorting out the terms containing the Grashof number and $\bar{\phi}$,

$$\bar{u} = -\ \mathrm{Re} + C_1\left[\frac{\mathrm{Gr}}{8}\left(\frac{\bar{y}^4}{3} - \frac{9}{10}\,\bar{y}^2 + \frac{7}{15}\,\bar{y}\right) + \frac{\bar{\phi}}{2}\left(\frac{3}{2}\,\bar{y}^2 - \bar{y}\right)\right] \tag{23}$$

$$\bar{T} = (1 + C_1\bar{x})\,\bar{y} + \frac{\mathrm{Pr}\ C_1^{\,2}}{240}\left[\frac{\mathrm{Gr}}{420}\,(100\bar{y}^7 - 567\bar{y}^5 + 490\bar{y}^4 + 99\bar{y}^3 - 122\bar{y}) + \bar{\phi}\,(9\bar{y}^5 - 10\bar{y}^4 - 3\bar{y}^3 + 4\bar{y})\right] \tag{24}$$

The pressure field can be found from an integration of either Eq. (5) or (6) and boundary condition of Eq. (13). We will decline from this derivation and focus on the implications of the predicted $\bar{u}$ and $\bar{T}$ fields.

Figure 3 shows the velocity profile given by Eq. (23) for three different values of the ratio $\mathrm{Gr}/\bar{\phi}$. This ratio is an indication of whether the gravity effects or the surface-tension effects dominate in the convection process. A pool of n-butanol of 0.02 m depth, supply temperature T_∞ = 299.7 K, will have a Gr of 6000. The surface-tension parameter $\bar{\phi} \approx -100$. Thus the $\mathrm{Gr}/\bar{\phi} = -60$ curve indicates the earth-based experiment while $\mathrm{Gr}/\bar{\phi} = 0$ is the zero gravity experiment. Also shown in the figure is the profile when $\mathrm{Gr}/\bar{\phi} \to -\infty$. Several interesting points are evident from Eq. (23) and Fig. 3.

1. Far ahead of the flame where no surface-tension and temperature gradients exist the fluid velocity will be unform $\bar{u} = -Re$. At smaller values of $\bar{x}$, the velocity profile is perturbed by the cooperative action of buoyancy and surface-tension effects in such a way that at about $\bar{y} = 1/3$ a velocity maximum in the negative x-direction would occur. With zero-gravity (i.e., with only surface-tension effect) this maximum occurs exactly at $\bar{y} = 1/3$ with $\bar{u}_{max} = -Re + C_1 \bar{\phi}/12$. As the gravity effects become relatively larger, the depth at which this maximum occurs will slightly decrease towards $\bar{y} \approx 0.274$ when $Gr/\bar{\phi} \to -\infty$ where $\bar{u} \approx -2.319$ Re.

At about $\bar{y} = 2/3$ (as at $\bar{y} = 0$), $\bar{u} = -Re$. With increasing Grashof number, this value of $\bar{y}$ where $\bar{u} = -Re$ will decrease towards about 0.59 as $Gr \to \infty$. At the surface $\bar{y} = 1$, $\bar{u} = \bar{u}_s = 2.33$ Re when $Gr/\bar{\phi} \to 0$ and $\bar{u} = \bar{u}_s \approx 1.121$ Re when $Gr/\bar{\phi} \to -\infty$. In general,

$$\bar{u}_s = \frac{Re}{3} \frac{\left(7\bar{\phi} - \frac{37}{140} Gr\right)}{\left(\bar{\phi} - \frac{11}{140} Gr\right)}$$

Another important feature of Fig. 3 is that As $Gr/\bar{\phi}$ gradually increases towards $-\infty$, the slope $\partial\bar{u}/\partial\bar{y}$ at the surface gradually decreases towards zero. This fact is quite evident from the boundary condition Equation (10).

2. In the present theory, the coefficient C_1 is independent of $\bar{x}$ as a result of the assumption $\partial\bar{T}/\partial\bar{x}$ is a constant with respect to $\bar{x}$. In an exact solution these quantities will be functions of $\bar{x}$. Then there exists a certain $\bar{x}$ at which

$$C_1 = \frac{4\ Re}{\left(\bar{\phi} - \frac{Gr}{20}\right)}$$

and where the local surface velocity $\bar{u}_s$ is zero. If $\bar{x}$ is larger than this certain stagnation point, fluid elements at the surface move towards the flame (i.e., in the negative x-direction) whereas behind the stagnation point, the surface velocity will be positive. It is this forward movement of fluid induced jointly by the surface-tension and gravity effects which would convect heat forward to enable the flame to spread.

3. The linearity of temperature with respect to $\bar{x}$ is not merely an ad hoc assumption. For unexplained physical reasons, this simple behavior has been clearly demonstrated by the detailed numerical solutions of Torrance [8,9]. This linearity makes the x-dependency of the velocity profile rather weak. As long as our region of interest lies within $0 \leq \bar{x} \leq -1/C_1$, the velocity profile retains a fixed shape; to the right of this domain, the velocity will be uniform and equal to -Re. The abruptness with which the linear temperature distribution would indicate the velocity field is a quirk of the present theory. This issue requires

further study.

4. Note from Eq. (23) that when the gravitational effects are absent, the functional form of the velocity profile is precisely that which has been obtained before by such authors as Levich [40], Adler [42], Yih [41], and Sirignano and Glassman [7].

5. Figures 4 and 5 show the temperature profiles of Eq. (24) for two different flame propagation Reynolds numbers. Three different Grashof numbers are considered in these plots keeping the liquid Prandtl number and surface-tension parameter constant. As stated earlier, a Gr of 6×10^3 refers to earth-based experiment on a 0.02m deep pool of a fuel such as butanol at room temperature. The maximum temperature attainable in the liquid layer is $\bar{T} = 1$ which occurs at the free surface $\bar{y} = 1$ near the flame's leading edge $\bar{x} = 0$. The lowest possible temperature is, of course, $\bar{T} = 0$.

Eventhough our theory considers the flow problem as fully developed, the temperature profiles indicate a boundary layer type development. Depending upon the conditions of Gr and Re, the thermal penetration occurs to a depth of $\bar{\delta}$ from the surface in such a way that for $\bar{y} \leq 1-\bar{\delta}$ the temperature $\bar{T}$ is zero. The magnitude of $\bar{\delta}$ depends on the distance ahead of the flame front. For $\bar{x} \geq \bar{x}_\infty$ ($\equiv -1/C_1$) the temperature profile is uniform and equal to $\bar{T} = 0$ (see Eq. (24)). At $\bar{x} = \bar{x}_\infty$, $\bar{\delta}=0$. As one moves towards $\bar{x} = 0$ from $\bar{x} = \bar{x}_\infty$ gradually, $\bar{\delta}$ would gradually increase.

An examination of Eq. (7) points out that if $\bar{u}$ were a constant, (say $\bar{u}_s$), similarity solutions must be possible for $\bar{T}(\bar{x},\bar{y})$ in such a way that $\bar{y}/\sqrt{[(\bar{x}_\infty-\bar{x})/Pr\ \bar{u}_s]}$ is the similarity parameter. In order to test this hypothesis, the calculations of Figs. 4 and 5 are examined to see how the depth of penetration would vary with $\bar{x}$. The result is as follows:

$$\frac{\bar{\delta}}{\sqrt{\left(\dfrac{\bar{x}_\infty - \bar{x}}{Pr\ \bar{u}_s}\right)}} = \text{constant}$$

The constant is given in Table III for the different Gr and Re. Remarkable is that the constant is about 6 for the two larger Grashof numbers irrespective of the Reynolds number. It is about 2.5 for Gr=0. Eventhough one would wonder if the use of the surface velocity $\bar{u}_s$ (which is a function of Gr, $\bar{\phi}$ and Re) in composing the similarity parameter is appropriate, the result is interesting. Further study of this aspect is required. Suffice it to note that under otherwise same conditions, the zero-gravity thermal field penetrates less deep into the fuel layer.

6. At a low flame propagation speed, as shown in Figure 4, a Gr of 10^5 results in a temperature field which is fully developed, i.e., the thermal penetration occurs all the way to the bottom of the pool. The profiles are nearly linear. Considerable heat losses may then occur to the base of the pool. At a medium Grashof number value ($\approx 6 \times 10^3$) the penetration occurs to the base but only close to the flame front. However,

TABLE III

TEST OF BOUNDARY LAYER HYPOTHESIS

$Pr = 45$ $\quad \bar{\phi} = -100$ $\quad (\bar{\delta} \equiv 1-\bar{y}_o,\ \bar{x}_\infty = -1/C_1)$

GR	Re	$\bar{\delta}\sqrt{\left(\frac{P_r\ \bar{u}_s}{\bar{x}_\infty - \bar{x}}\right)}$
10^5	2	- *
	10	6.04
$6x10^3$	2	5.94
	10	6.05
0	2	2.50
	10	2.77

*Fully developed thermal field.

at zero gravity, the maximum depth to which the thermal perturbations penetrate is only about a quarter of the pool depth.

7. A comparison of Figures 4 and 5 points out that while the general features of the thermal field remain changed, a faster propagating flame would result in a shallower penetration of the thermal disturbance. Even at the largest Gr considered, only the top half or so of the fuel layer will be influenced thermally. For lower Grashof numbers the temperature changes are limited to a thin layer of the fuel near the surface.

8. The surface temperature variation evident in Figures 4 and 5 is specifically presented in Figure 6. The linearity arises from our basic assumption. From $\bar{T}_s = 1$ at $\bar{x} = 0$, the temperature decays to $\bar{T}_s = 0$ at a value of $\bar{x} = \bar{x}_\infty = -1/C_1 = -3(\bar{\phi}-11Gr/140)/40$ Re. Larger Reynolds numbers, smaller surface-tension parameters and smaller Grashof numbers result in a shorter region of thermal perturbance. Especially the gravity level decreases the extent of the $\bar{x}$-region of activity by over an order of magnitude. This is an important result which would merit verification by experiments in the low-gravity. Figures 7 and 8 illustrate the variation of $\bar{x}_\infty$ with Gr, Re and $\bar{\phi}$.

9. The extent to which this theory is compared with experiments involves a comparison of the velocity profile and measurements of flame spread rate as dependent on Gr and $\bar{\phi}$. These are described in Appendix E. The measurements show that typically for alcohols, $\bar{\phi} \approx -100$ to 200,

Pr ≈ 45–100, Re ≈ 1–20, with Gr ≈ 6000. The results discussed above lead us to conclude that a 0.02 m fuel layer will experience thermal perturbation to a depth of 0.005 m at zero-gravity. The length $\bar{x}_\infty$ then is less than about 5 so that a physical length of 0.1 - 0.15 m is required to observe the region of thermal influence. Thus we can conclude that a tray of depth 0.02 m and length 0.4 m will suffice. As the experiments of Appendix E show, this length would permit exclusion of about 0.07 - 0.15 m for the ignition transient decay and 0.05 - 0.10 m for the alleviation of the upstream boundary effects.

APPENDIX D

Ignition of Fuel Pools that are Initially Below Their Flash Point

Consider a fuel pool whose initial temperature is below its flash point. Suppose an electrically heated wire, to be considered as a cylinder, is placed parallel to the pool surface at a distance D from the surface in the gas phase. Let the power ($\dot{q}'$ per unit length) be switched on at time zero. A transient free convection flow is thus initiated in the gas-phase surrounding the cylinder. A temperature field would develop to steady state in a short time. As the flow develops and thermal wave penetrates, a time will come beyond which the liquid surface gets into thermal contact with the heat source. Suppose that the gas phase thermal field around the ignition source is cylindrically symmetrical (as expected in the absence of gravity). Suppose then that the isotherm of significant influence on the surface is of diameter d, this isotherm cutting the quiescent liquid surface resulting in a segment of length d' which is the width of heated liquid surface strip. d' depends on D and d according to

$$d' = d \sqrt{\left[1-\left(\frac{2D}{d}\right)^2\right]}$$

As a result of this heating, a surface temperature gradient is established as one marches along the liquid surface normal to the ignitor. The consequent surface-tension gradient would initiate a convection process transiently forming a pair of symmetrically placed cylindrical flow cells. If $\dot{q}'$ were dispersed in the gas phase around the ignitor symmetrically, the fraction of $\dot{q}'$ delivered to the liquid is given by

$$f = \frac{2}{2\pi} \sin^{-1} (d'/d)$$

Given this situation, to determine the flow patterns, the heat transfer distribution, the resultant production of fuel vapors, their dispersion in the gas-phase and ignition of the mixture so formed consitute an important problem both in science and practice.

Our considerable search into the engineering, physics and chemistry literatures pointed out only a few references to this problem [2,4] all from Princeton. We therefore develop in the following a brief analysis to identify the process components of the problem.

The quantity of energy $f\dot{q}'$ delivered to the liquid is transported away by convection. The fluid velocities both in the x and y directions, u and v, are of the same order of magnitude in this ignition problem. The convective transfer of energy hence is described by

$$f\dot{q}' = d' \rho u C_p (T-T_\infty) \qquad (1)$$

where d' is the area of incident heat per unit width of the pool, $\rho u \approx \rho v$

is the liquid mass flow rate, C_p is specific heat of the liquid of initial temperature T_∞. T is the time- and space-dependent temperature of the liquid fuel. The velocity u is dependent on time and space as well. Assuming that the flow and thermal fields react instantaneously to the influence of the ignitor-heating, we assume that $u \approx u_s$, the x-directional velocity at the free surface of the fuel. From the flame spread theory (Appendix C, Eq. (23)).

$$\bar{u}_s = \frac{-C_1}{4}\left(\frac{Gr}{20} - \bar{\phi}\right) \tag{2}$$

Here $\bar{\phi}$ is the sensitivity of surface tension to the fuel temperature $d\bar{\sigma}/d\bar{T}$. Implicit in Eq. (2) is that the surface temperature is representative of the convective dispersion intensity of energy. Substituting Eq. (2) in Eq. (1),

$$f\dot{q}' = d'\rho C_p\, u(T-T_\infty) \approx d'\rho C_p\, u_s\, (T_s-T_\infty) \tag{3}$$

which becomes

$$\bar{T}_s \frac{d\bar{T}_s}{d\bar{x}} = \frac{-\bar{q}}{\bar{d}\left(\frac{Gr}{20} - \bar{\phi}\right)}$$

with the nondimensional quantities defined in Table II. Integration with $\bar{T} = 0$ at $\bar{x} = \bar{\Delta}$ gives

$$\bar{T}_s = \left[\frac{2\bar{q}(\bar{\Delta}-\bar{x})}{\bar{d}\left(\frac{Gr}{20} - \bar{\phi}\right)}\right]^{1/2} \tag{4}$$

The $\bar{x}$-directional extent of thermal penetration $\bar{\Delta}$ is an indication of the cell dimension, an yet undetermined function of time. Before further dealing with this quantity, the temperature averaged over $\bar{x} = 0$ to $\bar{\Delta}$ is obtained from Eq. (4) to be

$$\bar{T}_{av} = \frac{2}{3}\bar{T}\Big|_{\bar{x}=0} = \frac{2}{3}\left[\frac{2\bar{q}\bar{\Delta}}{\bar{d}\left(\frac{Gr}{20} - \bar{\phi}\right)}\right]^{1/2} \tag{5}$$

As the energy is thus convected, it is employed to heat two approximately cylindrical masses of liquid of diameter Δ and of temperature $\approx T_{av}$.

$$f\dot{q}' \approx 2.\ \frac{\pi\Delta^2}{4} \cdot \rho C_p \frac{dT_{av}}{dt} \tag{6}$$

The factor 2 on the right hand side is to account for the two symmetrical cells. $\pi\Delta^2/4$ is the volume of the cell per unit width of the pool. With the nondimensional time $\bar{t}$ defined in Table II, Eq. (6) becomes

$$\bar{q} = 2\pi\bar{\Delta}^2 \frac{d\bar{T}_{av}}{d\bar{t}} \tag{7}$$

From Eq. (5) the temperature-time derivative is

$$\frac{d\bar{T}_{av}}{d\bar{t}} = \frac{1}{3}\left[\frac{2\bar{q}}{\bar{d}\left(\frac{Gr}{20}-\bar{\phi}\right)}\right]^{1/2} \bar{\Delta}^{-1/2} \frac{d\bar{\Delta}}{d\bar{t}}$$

with which, Eq. (7) may be rewritten as

$$\bar{q} = \frac{2\pi}{3}\left[\frac{2\bar{q}}{\bar{d}\left(\frac{Gr}{20}-\bar{\phi}\right)}\right]^{1/2} \bar{\Delta}^{3/2} \frac{d\bar{\Delta}}{d\bar{t}}$$

Upon integration with the initial condition that there exists no cell ($\bar{\Delta} = 0$) at $\bar{t} = 0$,

$$\bar{\Delta} = \left[\frac{15\bar{t}}{4\pi}\right]^{2/5} \left[\frac{\bar{d}\bar{q}\left(\frac{Gr}{20}-\bar{\phi}\right)}{2}\right]^{1/5} \tag{8}$$

Equation (4) in conjunction with Eq. (8) gives the surface temperature as a function of $\bar{x}$. Equation (5) gives the average temperature of the cell to depend on time as

$$\bar{T}_{av} = \frac{2}{3}\left[\frac{15\bar{t}}{4\pi}\right]^{1/5} \left[\frac{2\bar{q}^{3/2}}{\bar{d}\left(\frac{Gr}{20}-\bar{\phi}\right)}\right]^{2/5} \tag{9}$$

From Eqs. (2) and (4) the surface velocity is

$$\bar{u}_s = \frac{1}{4}\left[\frac{\bar{q}\left(\frac{Gr}{20}-\bar{\phi}\right)}{2\bar{d}(\bar{\Delta}-\bar{x})}\right]^{1/2} \tag{10}$$

Equations (4), (8), (9) and (10) give a detailed structure of the transient flows developed in the ignition process. Ignition is expected to occur when the temperature at $\bar{x}=0$ reaches the fuel's flash point temperature T_o. Thus setting $\bar{T}=1$ and $\bar{x} = 0$ in Eq. (4), with $\bar{\Delta}$ given by Eq. (8), the ignition time $\bar{t}^*$ is obtained.

$$\bar{t}^* = \frac{4\pi}{15}\left[\frac{\bar{d}\left(\frac{Gr}{20} - \bar{\phi}\right)}{2\bar{q}^{3/2}}\right]^2 \tag{11}$$

The extent of the cell at this time is

$$\bar{\Delta}^* = \left[\frac{\bar{d}\left(\frac{Gr}{20} - \bar{\phi}\right)}{2\bar{q}}\right] \tag{12}$$

Since for typical alcohols $\bar{\phi}$ lies in the range -100 to -200, $\bar{q} \approx 1.5$-15 (for $\dot{q}' \approx 10^{-1} - 10^{0}$ kw/m, $f = 0.5$), $\bar{d} \approx 0.04 - 0.20$, Δ^* will be about 0.33 - 15 cm, $t^* \approx 0.125 - 10^3$ sec. at zero gravity and $\Delta^* \approx$ 10-15 cm and $t^* \approx 1$-10^3 sec at normal gravity.

In Figure 9, the predicted dependency of $\bar{t}^*$ and $\bar{\Delta}^*$ on Grashof number and surface-tension parameters are shown especially attempting to point out the influence of reducing gravity to zero. Notable qualitative agreement is obtained between this theory and the experimentally observed flow patterns. Implicit in both the flame spread theory of Appendix C and Ignition theory of this appendix, we must stress, is the assumption of negligible hydrostatic depression of the liquid layer free surface. The impact of this assumption can be best assessed by comparison of normal gravity data and results obtained by experimentation in Spacelab.

APPENDIX E

Experimental Work

The experimental part of our project was intended to check some of the theoretical predictions related to the feasibility and justification issues. These issues pertain to the dimensions of the pool, the choice of fuel, possibility of using inert liquids to examine the physics of flow, the choice of flow tracers, etc.

1. Preliminary Experiment: Our preliminary experiments involved a simple cast iron tray of constant width and one meter length. Washed sand was placed in the tray to produce a flat inclined bottom such that when the tray is filled with liquid fuel, the pool depth varied linearly along the length of the tray with zero depth on one end and 3.2 cm on the other. Some interesting observations were made with this apparatus.

(i) When ignition was attempted by bringing a match flame to the vicinity of the liquid surface, ignition was found to be extremely difficult in the deep end. This is because of the excessive energy dissipation into the liquid phase as a result of strong circulation of the fluid produced by the surface-tension effects. Ignition in the shallow end, however, would occur readily, perhaps because of the suppressed liquid motion.

(ii) Once ignition is accomplished in the deep end, even if with some difficulty, the flame would propagate towards the shallower end, first steadily and then in a somewhat faltering way. A flame initiated easily on the shallower end, however, would propagate but infinitesimally slowly; for all practical purposes, the flame burns there over a wick formed of the sand.

(iii) If ignition is attempted somewhere in the middle of the pool length, the deeper the pool the more difficult the ignition and the easier the flame spread.

These simple experiments pointed out the importance of surface-tension-driven liquid convection which plays opposing roles in ignition and flame spread. In ignition, it disperses energy away thus delaying the arrival of the instant when the liquid would produce enough vapors conducive to ignition. In spread, the convection offers the controlling forward heat transfer mechanism. A critical depth of about 2.5 cm was discovered in our preliminary experiments to permit formation of a convection cell which is unhampered by the lower solid boundary of the pool. This observation appeared to be independent of the particular fuel under test.

2. Choice of Fuel: The tested fuels include kerosene, xylene, ethanol and butanol. Among these, kerosene is the only fuel which is a mixture of several basic hydrocarbon fuels. Even though the various other

fuels have a stated purity (ex: 95% pure, tech. grade, or reagent grade, etc.) the impurity in most cases is caused by the presence of different isomers of the same molecular formula. Our constraints in the choice of the fuel included: easy availability, safety in view of toxicity, cleanliness in terms of sootless burning, lack of corrosivity, etc. Choice of a fuel which burns without soot is also desirable in view of reducing the effects of radiant heat transfer in flame spreading. And, of course, the fuel has to possess a relatively strong dependence of surface-tension on temperature. The flash point temperature has to be larger than the room or fuel supply temperature to accentuate the role played by surface-tension but not so large as to yield a pulsating precursor flame in the flame spread experiment.

Our experiments rapidly pointed out that xylene (and other fuels with cyclic structure) are undesirably corrosive to the pool pan and the associated sealants. Kerosene is too commercial a mixture to have well-documented properties. Ethanol and some other fuels are too close in flash point to the fuel supply temperature. Decane is too expensive to permit repetitive experimentation. With these observations, n-butanol has been chosen as our test fuel.

3. Tray construction: Figure 12 shows the detailed construction of the fuel tray for the majority of experiments. Trays are fabricated of 0.080 gage aluminum in such a way that the side walls are only 1/2" high. 1/8" thick plate glass walls are then inserted in place with silicone sealant applied between the glass and aluminum to avoid fuel leaks. In some tests, the silicone sealant was replaced by a folded teflon tape and the glass walls are press-fitted. Xylene fuel attacks the silicone sealant seriously and the teflon tape less seriously. Six different widths ranging from 1/2" to 4" are thus accomplished for the finished pool trays. All the trays are 48" long except the smallest one which is 24" long. All are 2" deep. The end walls of all trays are unlined aluminum. Each tray is provided with fitting false bottoms which are also fabricated out of aluminum; these are to provide a variable depth to the pools while at the same time resulting in a solid bottom.

MacKinven et al [6] employed a substrate layer of water over which the fuel is situated in the desired thickness. The solid bottom arrangement chosen in our experiments is expected to eliminate difficulties of stipulating the velocity and thermal boundary conditions at the base in the theoretical analysis.

A screw-hole was tapped in the bottom of each tray to accommodate a machine screw, removal of which after a test facilitates emptying the pan into a spent-fuel reservoir. A 15 cm ruler was situated in the background for obtaining the temporal location of the spreading flame front from video records. This entire tray set up was placed inside a 4' x 4' by 8' long test chamber to avoid spurious drafts and to keep under control the combustion products. Various lighting distributions and backgrounds are employed to obtain the best records of fuel convection patterns photographically and via video taping.

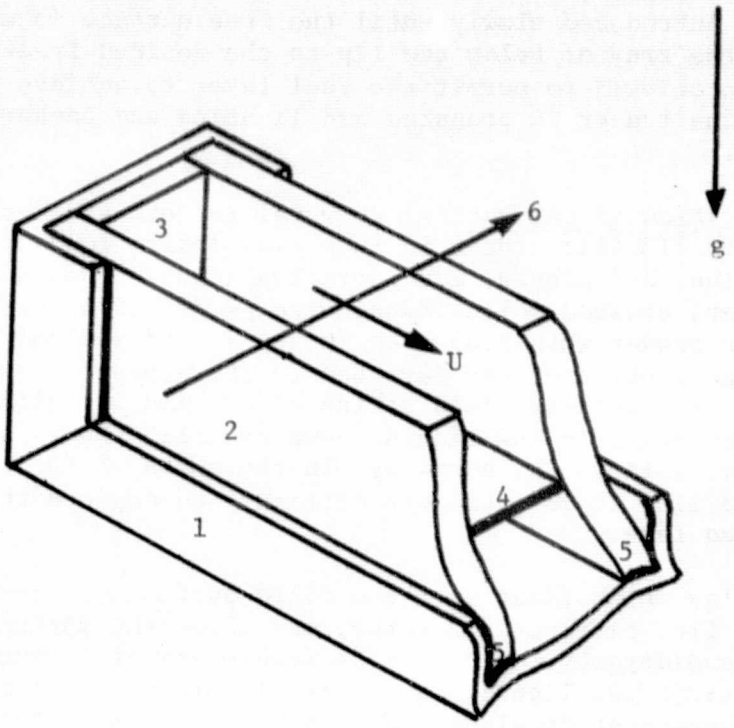

1. Aluminum tray frame
2. Side glass
3. End glass
4. False bottom
5. Silicone seal
6. View line

FIGURE 12: TRAY CONSTRUCTION DETAIL.

In a few experiments, a copper tube coil, carrying water at a chosen temperature, is placed in the space under the false bottom in order to achieve a prescribed initial temperature of the fuel. Due to difficulties associated with achieving a steady uniform temperature of the fuel by thus cooling or heating, the scheme is aborted in later experiments.

4. Procedure. Typically, upon setting up the tray of certain width in place, the false bottom is installed to obtain the desired fuel depth. The fuel is introduced slowly until the free surface is either flush with the lip of the tray or below the lip to the desired free-board. Sufficient time is then allowed to permit the fuel layer to achieve quiescence during which time the tracer is prepared and lighting and background adjusted for photography.

a. Flow Visualization: Several tracers are tested for flow visualization [13,44]: these include dyes (milk, food coloring, ink, methylene blue, and others) and particles (dust, crushed aluminum shavings, talcum powder, crushed polystyrene, fine powder of asbestos, and others). The asbestos powder when dispersed in the liquid yielded an unexpected effect. Fine bubbles of air desorbed by the asbestos rise in the liquid in the form of a string. This string of bubbles is deflected by any disturbing currents in the liquid, however mild. Whereas a string of bubbles is visible to the naked eye in the shape of the local instantaneous velocity profile, it is extremely difficult to capture this profile on film or video tape.

Particles which float over the fluid surface are excellent to observe the surface flow patterns. But they may alter the surface-tension phenomena considerably. The most desirable tracer is one which is neutrally buoyant in the liquid and yet is visible to the eye and camera. We have discovered that finely ground chalk or talcum of the color of one's choice (purple and blue appeared to us desirable) when soaked overnight in the fuel of concern (in such proportions as about 5% talcum to 95% fuel) would form a fine paste whose properties are expected to be similar to those of the fuel itself. This slurry could be applied to a quiescent pool of fuel with an eye-dropper specially equipped with a fine wire to convey the slurry to the liquid with least resultant inertial disturbance. This is the tracer technique we have chosen to employ in most of our experiments.

b. Ignition Methods in the Flame Spread Experiment: Three different methods of ignition are employed in the flame spread experiments. The simplest and the most extensively used one involves bringing a kitchen match flame close to the fuel surface ($\approx$ 0.5 cm separation) and holding it there until ignition would occur. This method has the merit of producing the least amount of disturbance in the gas and liquid phases. But it also has the shortcoming of being ineffective when the flashpoint of the fuel is much higher than the supply temperature. To handle this situation, the second method is developed. In this, a small quantity of low flash point fuel such as methanol is gently released on to the test fuel surface at one end of the tray to form a thin floating layer which can be ignited easily with a match flame. If the quantity of accelerant

released is large enough, the test fuel ignition occurs quite smoothly and a spreading flame evolves. In the third method, which is the least used in our experiments and which is meant for situations requiring considerable quantity of the accelerant because of large differences between the flash point and supply temperatures, a solid barrier flag fabricated out of masonite is employed to contain the relatively massive accelerant layer from spreading over the test fuel surface. Upon ignition of the accelerant, the barrier is gently removed. The liquid is expected to be disturbed to some extent during this removal, no matter how gently it is carried out. Whereas the mode of ignition did not cause any significant differences in the flame spread measurements in the 48" long trays, it is expected that the first method is the least disturbing and the third method is the most disturbing to the condensed phase quiescence. Correspondingly, the portion of the tray length influenced by the transience of ignition is expected to be largest in the third method.

c. Heat Source in the Ignition Experiments: Two different heat sources are employed in the study of preignition flow patterns in the liquid. A heated nichrome wire of diameter 0.08 mm (B&S gage 40, resistance $\approx$ 2.3 ohms/cm) is placed in the direction of width between ceramic terminals. The distance between the wire and liquid surface can be accurately adjusted. The advantage of this method is that the power input can be prescribed quite accurately. The disadvantage lies in that for any significant thermal communication between the relatively thin heated wire and the liquid surface, the wire has to be brought quite close to the surface, so close that even minor disturbances and vibrations in the building would cause the liquid fuel to touch the wire whereupon the surface-tension would keep the wire in continuous contact with the liquid.

To overcome this difficulty, a propane gas diffusion flame fed by a feeble flow of the gas through a 1/16" dia. copper tube is devised. The resulting flame is blue; its size can be adjusted from about 5 mm to 10 mm, with its length about 5 times the diameter; it can be brought close to the fuel surface; there exists a thermal communication between the nearly spherical bottom-half of the flame and the fuel surface even at such large separation distances as about 10 mm. The power input rate and flame size are controllable by adjusting the fuel flow rate but some ambiguities arise due to the incomplete combustion, a severe characteristic of all diffusion flames. In most of our pre-ignition flow studies, the gas flame ignitor was employed.

5. Results and Discussion: In the following, the results of experiments are presented first on flame spread and then on ignition and their implications are examined in our concern of the feasibility issues.

(a) General Observations: With all fuels the flame spread is smooth only in a certain range of supply temperature. For butanol this range is between 27.7 ^{o}C and 37.7 ^{o}C. If the supply temperature is lower than about 27 ^{o}C, the flame would propagate with pulsations, its leading edge propagating ahead to 2 or 3 centimeters and then withdrawing back.

To measure the flame speed consistently is nearly impossible when these pulsations occur. If the fuel temperature is greater than about 37 ^{o}C, the flame propagation is extremely fast ($\approx$ 50 cm/s). Meaningful observations of the liquid and gas phase processes are again extremely difficult.

In the intermediate range of supply temperature (27.7 to 37.7 ^{o}C) the flame would propagate in an orderly and uniform fashion permitting careful observations. Normally the flame fronts in 4" wide pools are nearly flat with parabolic shape as the sidewalls are approached. The liquid phase convection is clearly visible both by bubble tracers and talcum paste tracer. Typical velocity profiles in the liquid phase obtained by this later technique are consistent with what is expected from the hypothesis of Appendix C related to the induction of a surface-tension-driven flow.

In study of the motion of liquid in preignition heating, flow fields are obtained in a similar way. Because of the irregularities produced by the surface-tensional attachment process between the wire and the liquid surface, we have aborted the idea of using heated wire as ignition source and resorted to employing a 5 mm dia. propane diffusion flame for the purpose. Depending upon the separation distance between the blue flame (bottom part) and the liquid surface, a transient convection cell is developed.

(b) Influence of the Tray Construction Details: MacKinven [6] pointed out that the glass liners along the sidewalls of the tray resulted in a consistently larger flame spread velocities compared to the velocities obtained in unlined aluminum trays. This is expected to be due to heat losses to the side walls from the propagating flame and convected fluid. We expect, as evident from the remarks below in relation to the pool width effects, that these heat loss effects will have to be taken into account in a comprehensive theoretical program to develop a correction factor which would enable inference of flame spread in an infinitely wide tray from spread rates in trays of finite width.

That the end walls are bare aluminum surfaces is deemed irrelevant so far as our ignition and flame spread studies are concerned.

(c) Room Conditions: Most of the experiments reported here are conducted during spring and summer of 1978. The atmospheric pressure and humidity appear to be of no measurable consequence on the flame spread rate. The atmospheric temperature, however, appears to influence the spread rate via the fuel supply temperature. The reason for this is that the fuel is stored in a cabinet in which the temperature is essentially the same as that of the room.

(d) Fuel Type: The nature of fuel effects the flame spread velocity strongly at a fixed supply temperature in a given pan. At an initial temperature of 20.5 ^{o}C, in the 5.08 cm wide 90 cm long pool with

a fuel depth of 2.54 cm, the flame spread rates for xylene, kerosene and butanol are respectively 2.8, 0.6 and 1.2 cm/s respectively. The flash point temperatures (open cup) of these fuels are respectively 23.8, 49, and 43 °C. Mixtures of kerosene and xylene are also tested in the same tray keeping the initial temperature 21 °C ± 3%. The measurements are presented in Figure 13. The decrease in flame spread with increase in kerosene content of the mixture is not quite linear.

Another set of data obtained on butanol has the objective of determining the influence of fuel purity on flame spread rate. Figure 14 shows the spread rate as a function of the supply temperature for fresh butanol and for previously used butanol. There are obviously some significant differences, especially at lower temperatures. The spent fuel flame spread rate is, in general, lower than the fresh fuel flame spread rate. The video records lead us to believe that the surface-tension-driven currents in the liquid phase are not as intense in the spent fuel as in the fresh fuel. Ignition by match flame appeared to be a bit easier with spent fuel than with fresh fuel.

These observations lead us to believe that the spent fuel surface tension σ and its sensitivity to temperature $d\sigma/dT$ are lower than the same for fresh fuel. During combustion, the fuel surface is expected to encounter such products of combustion as soot and water vapor which are readily absorbed by the fuel. Knowing that even minor quantities of impurities in the fuel would enormously change the surface-tension characteristics, the observed lower flame spread rate and easier ignition of spent fuel are both logically expectable.

Finally, it is interesting to note that xylene is found in our experiments to be rather undesirably corrosive, even to silicone sealant, to such an extent that an uncontrolled spill fire hazard had arisen.

(e) Fuel Supply Temperature Effect: Figures 15, 16 and 17 present the influence of the fuel's initial temperature on the flame spread rate in trays of different widths and different fuel layer depths. Evident from these figures is that the flame spread rate increases from about 1 cm/sec at low temperatures to over 100 cm/sec at temperatures approaching the flash point (43.3 °C). The sensitivity of spread velocity to variations in fuel's initial temperature is much stronger at higher temperatures than at lower temperatures. This relationship appears to be nearly exponential. For fuel temperatures above 38 °C or closer to the flash point, the flame propagation is so fast that even the motion picture records yield data with a great deal of scatter.

(f) Free-Board Height Effect: The experiments reported here are all conducted with the fuel filling the tray nominally to 100% full; i.e., the fuel surface is nominally at the top edge of the tray walls. The nominal qualification is made to recognize that the fuel surface may be curved due to the surface-tension wetting of the walls. Nevertheless, the trays are so filled as to maximize the fuel loading without permitting spillage over the edges both before and during the flame spread.

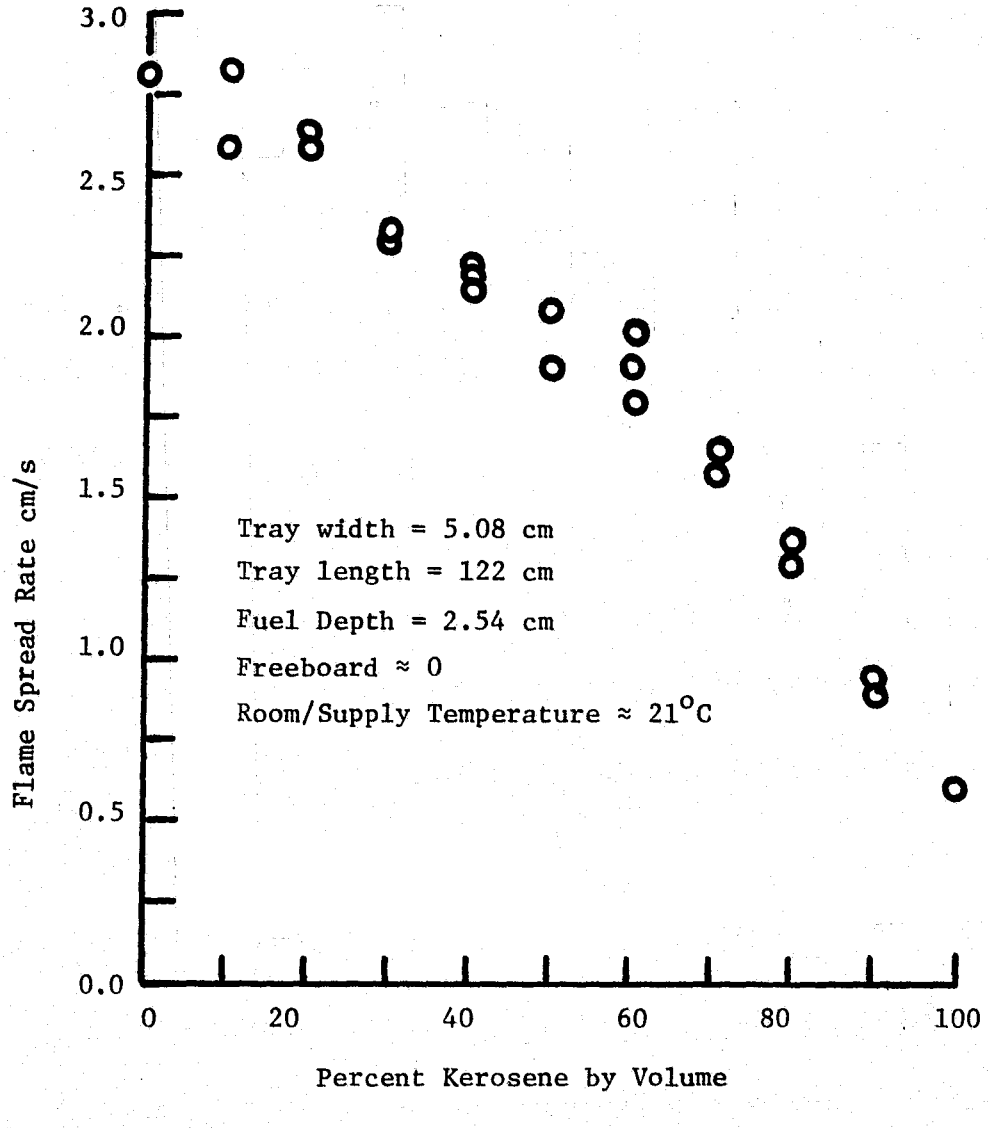

FIGURE 13: FLAME SPREAD RATE OVER LAYERS OF XYLENE + KEROSENE MIXTURES.

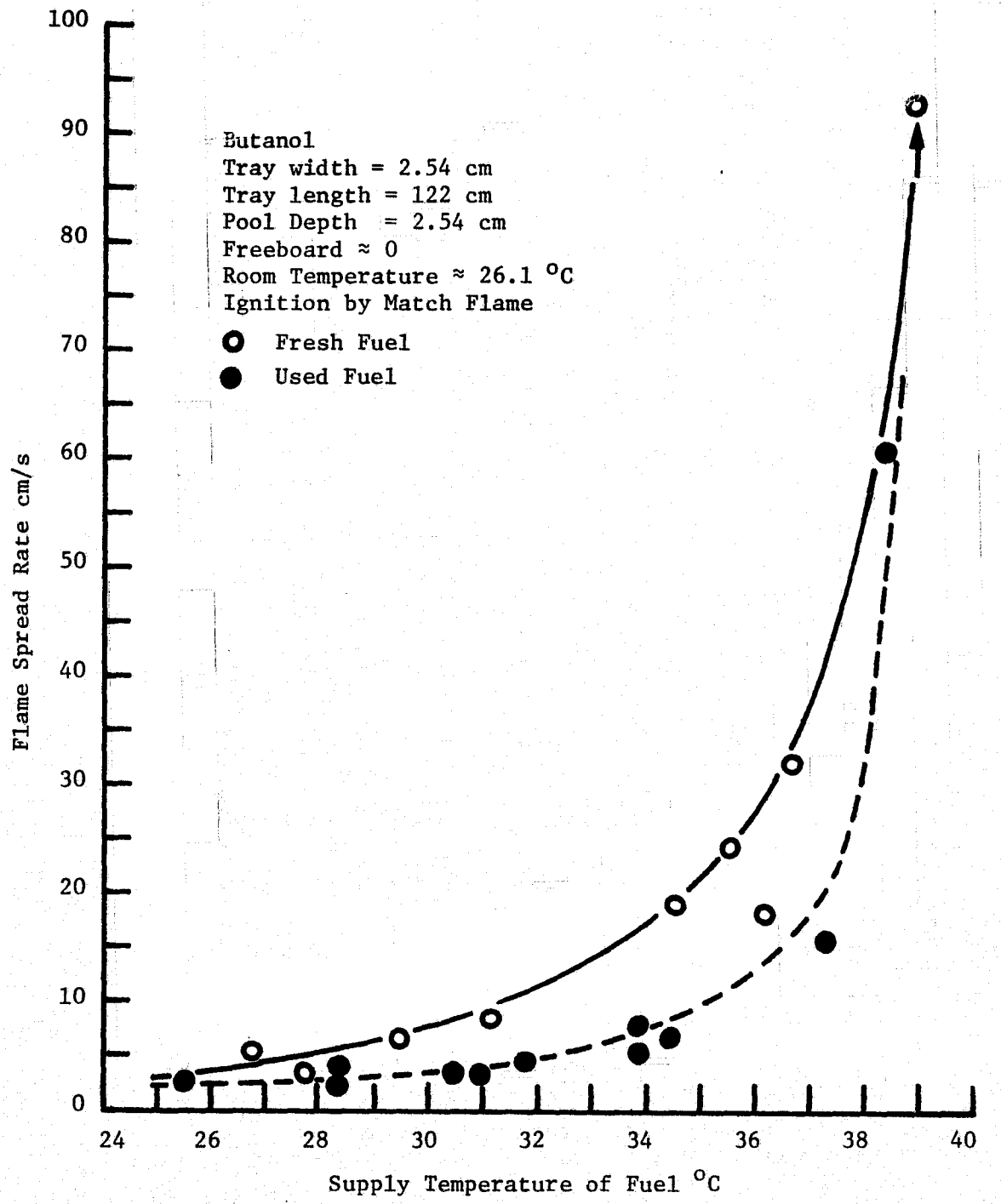

FIGURE 14: FLAME SPREAD RATE AS DEPENDENT ON PURITY OF BUTANOL.

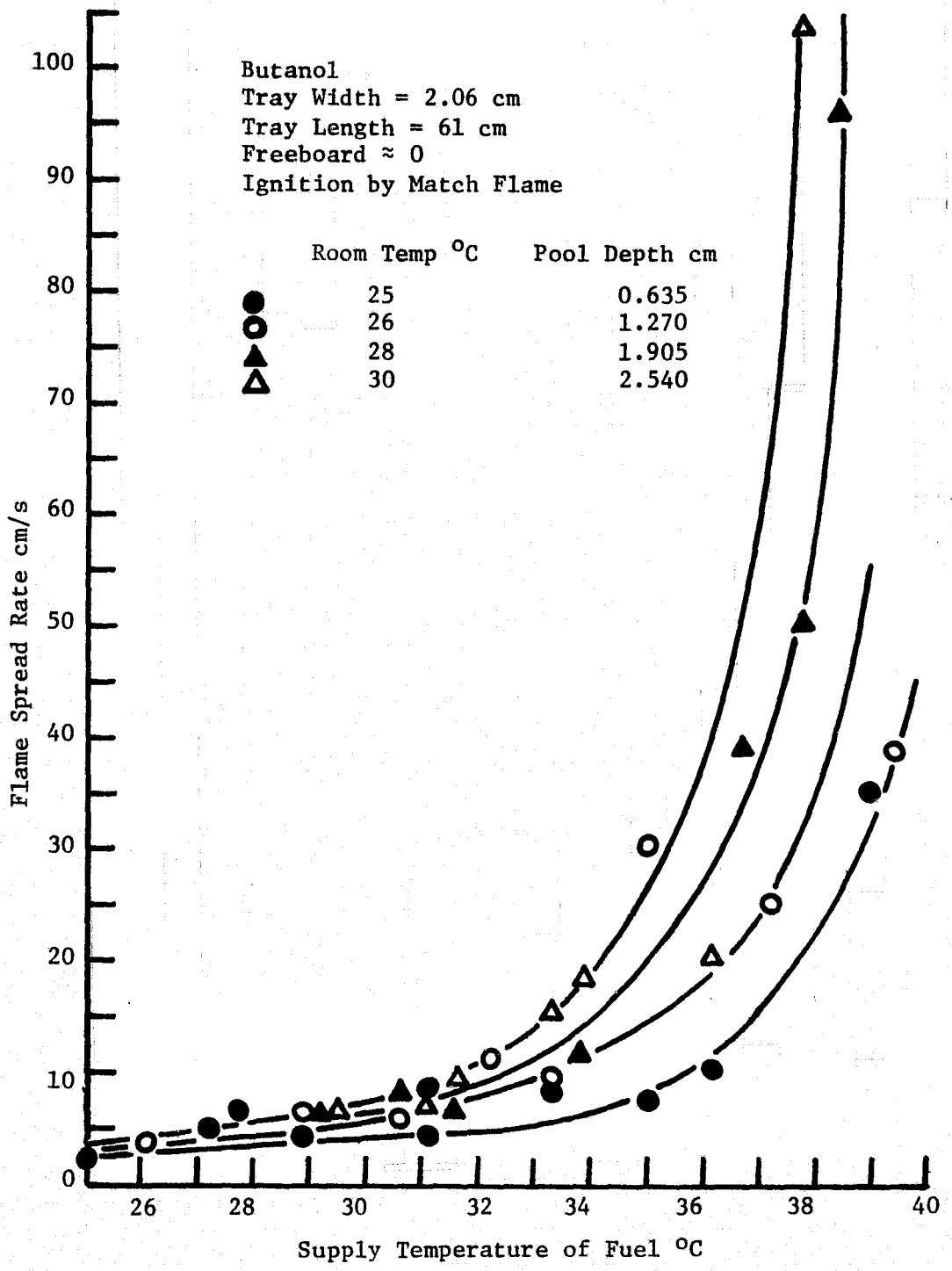

FIGURE 15: FLAME SPREAD RATE AS DEPENDENT ON SUPPLY TEMPERATURE AND POOL DEPTH.

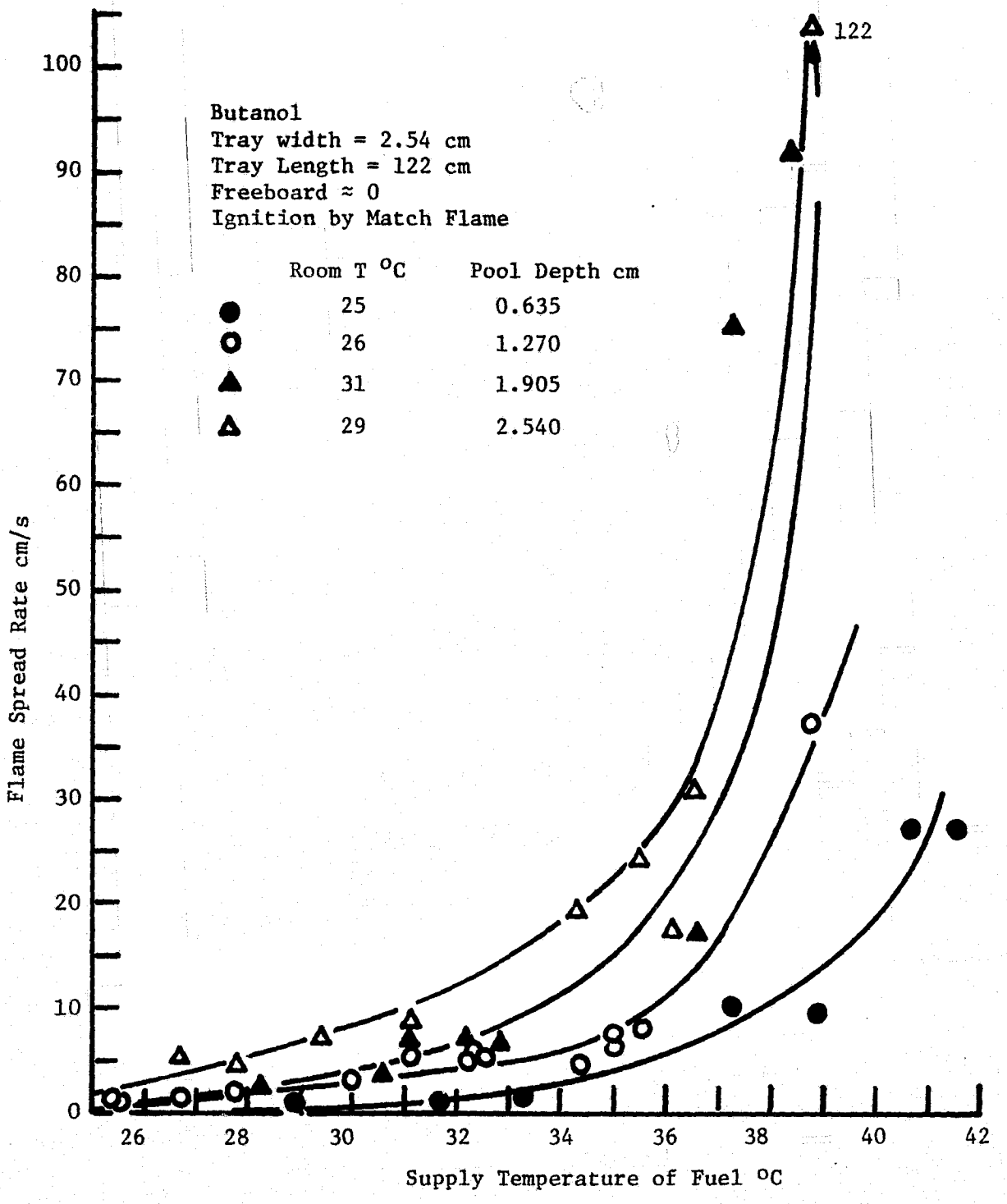

FIGURE 16: FLAME SPREAD RATE AS DEPENDENT ON SUPPLY TEMPERATURE AND POOL DEPTH.

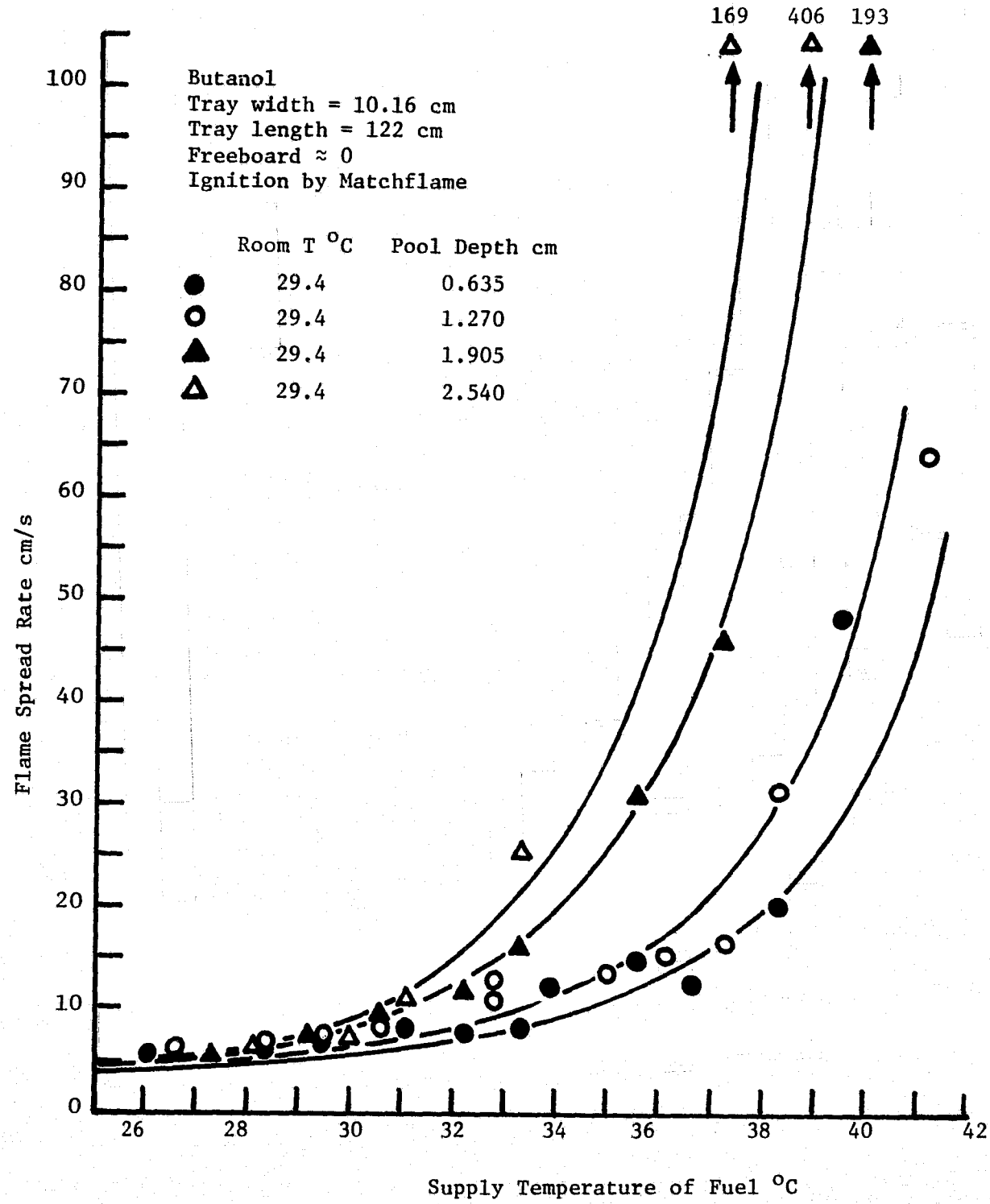

FIGURE 17. FLAME SPREAD RATE AS DEPENDENT ON SUPPLY TEMPERATURE AND POOL DEPTH.

The issue of how full is full is relevant in the viewpoint of not only the fire safety in the conduct of this experiment but also the energy feed forward mechanism itself. If the tray is only partially full, heating of the exposed part of the side walls, (the height of this exposed part being called 'free-board'), is expected to alter the mechanism of heating the fuel. Furthermore, the flame propagation in a partially filled tray would essentially resemble propagation in a narrow channel. The side walls then are expected to restrict the arrival of oxygen to the vapor and thus alter the flame spread characteristics.

The net effect of the heat transfer and air flow patterns altered by the free-board walls according to MacKinven's experiments [6], is to reduce the flame spread velocity. As the free-board height is increased from 0 (i.e., fuel surface flush with the top of the trays walls) to about 6 mm, the flame spread rate falls sharply. Further increases in free-board does not significantly influence the spread rate.

(g) Effect of Tray Width: The data of Figures 15 to 17 also indicate the effect of tray width on flame spread rate. Figure 18 is a cross-plot of these data at one particular depth of the pool, viz: 2.54 cm. The points in this figure are not necessarily actual data points but readings from Figures 15 to 17. In general, the trend is an increase in the spread rate with an increase in the tray width, presumably due to decrease in fractional heat loss to the side walls from the liquid and due to the viscous effects in the liquid at the side walls which alter the liquid phase energy convection process. When the flame temperature is low, e.g.: 30 ^{o}C, the pool width appears to be relatively inconsequential except in the narrowest configurations. At higher fuel supply temperatures, however, the effect of tray width is felt over the entire range of our testing. Similar experiments by MacKinven [6] indicate that a tray has to be as wide as 60 cm before one can neglect the effects of the finite width on spread rate.

Whereas the width of the tray produces marked change in the nature of the flames behind the spreading front, the leading edge of the flame appears to be early unaffected. (For narrow trays, the flame is laminar and its height is about 4-5 times the tray width. For the 10 cm tray, the flame appears to be turbulent and its height is about 2-3 times the tray width.) An estimation of the radiant heat transfer from the flames of different heights and of different characteristics is not made.

Even though Figure 18 is prepared for a pool depth of 2.54 cm, the general features described above are valid for other depths as well.

(h) Effect of Pool Depth: This is perhaps the most important effect which requires study both in theoretical and experimental view points. The reason for this importance is in the fact that in shallow pools the surface-tension-driven convection may become suppressed and hence the flame spread rate may be greatly reduced. Figure 19 shows the data cross plotted from Figures 15 to 17 at the narrowest width tested. Once again the points are not necessarily actual measurements but

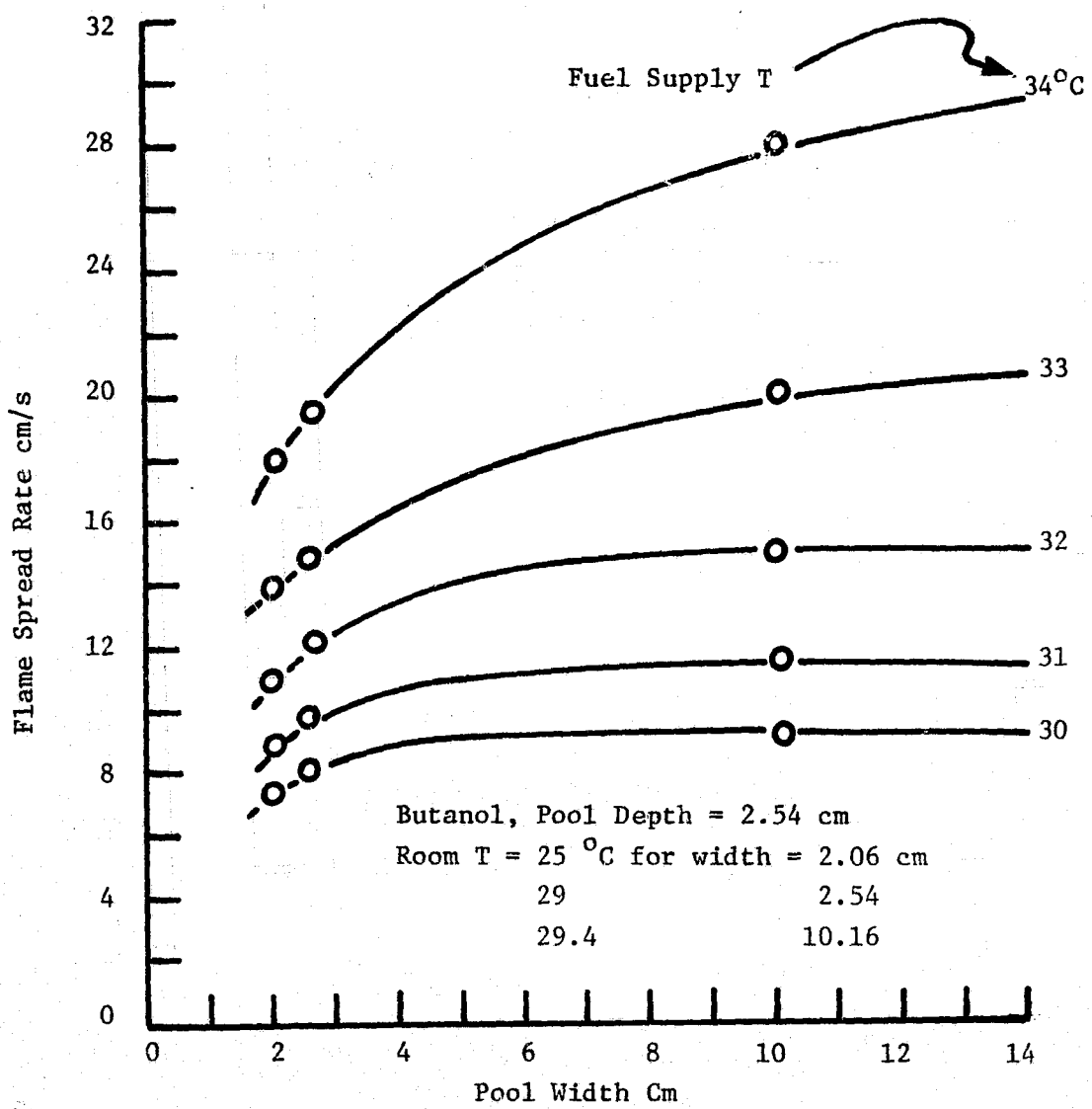

FIGURE 18: EFFECT OF POOL WIDTH ON FLAME SPREAD RATE.

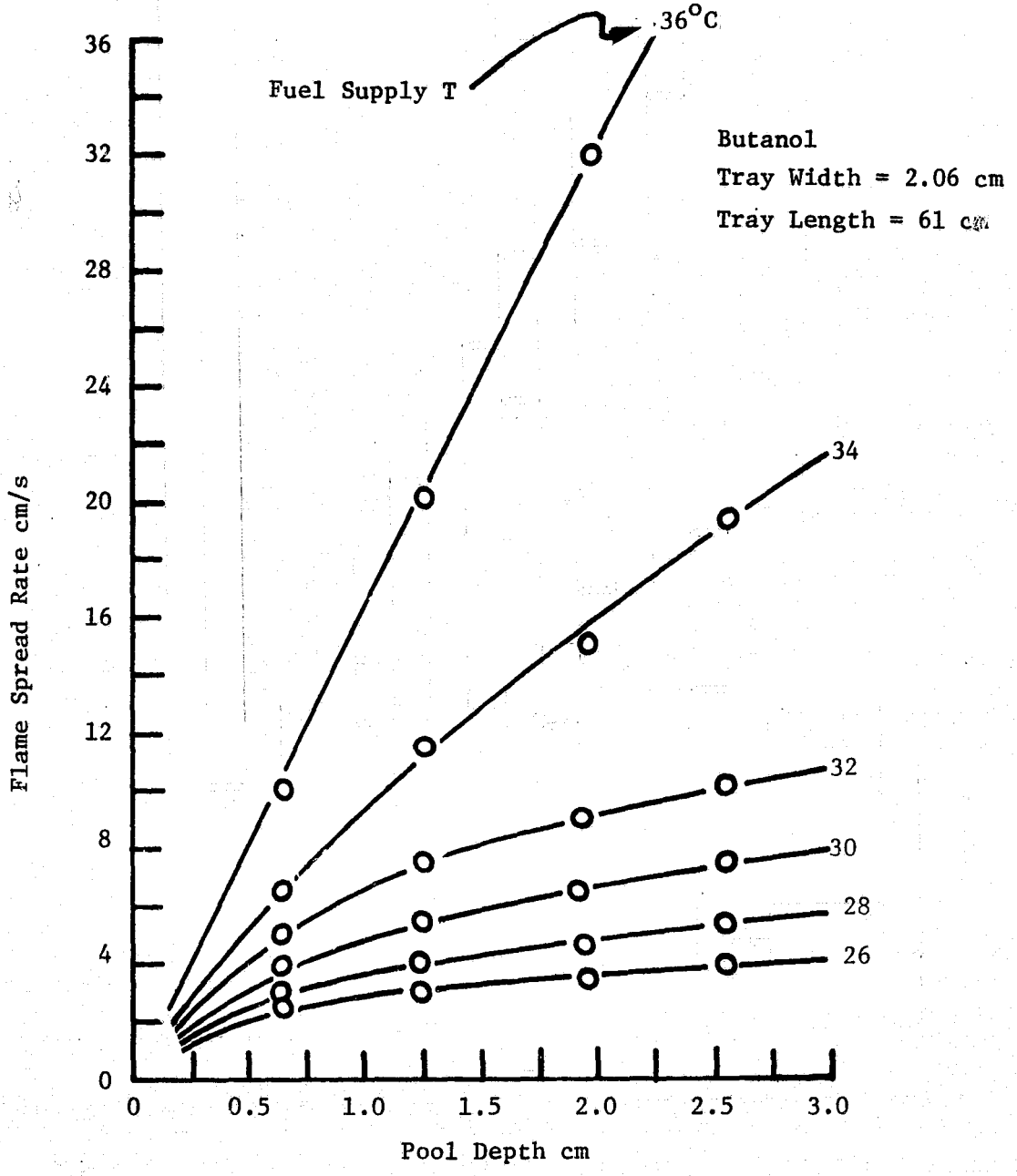

FIGURE 19: EFFECT OF POOL DEPTH ON FLAME SPREAD RATE.

but readings from the reference figures.

When the pool is about 1 to 2 mm deep, ignition may be possible but flame spread is not possible except when the fuel temperature is near the flash point. MacKinven [6] points out the reasons for the observation as (i) the excessive heat losses by conduction to the base of the tray and (ii) the suppression of the essential heat feed-forward mechanism of surface-tension-driven flow.

At larger depths, the spread rates are correspondingly larger. For depths greater than about 6 mm, the flame spread rate increases with pool depth nearly linearly the slope being larger at higher fuel supply temperatures. Estimates show that the heat loss rate to the base of the pool becomes negligible for depths beyond about 1.5 cm.

(i) Miscellaneous Observations: The flame spread experiment is conducted in trays of two different lengths, 122 cm and 61 cm. In almost all the cases, the fuel employed, namely butanol, permitted ignition by a simple exposure to a kitchen match flame. Based on the video records and visual observations, one can safely conclude that the ignition transient has extended no more than about 10-15 cm from the ignition end. In this length, there were observed liquid phase disturbances due to the preignition heat transfer. Once the flame is initiated and is spread over this length, a steady state is attained. All the flame spread rates reported above are taken from the flame location versus time data in the middle 1/3 of the length of the tray. As the flame would propagate over the length of the tray and approach the far end of the pool, the end walls are expected to effect the surface-tensional convection and thus effect the flame spread. From an estimation of the dimension of the convection cell, we conclude that the last 10 cm or so of the pool length will result in a flame propagation altered by the presence of the end wall.

6. Observations in the Preignition Heating Experiments: As a propane flame is brought into the vicinity of a quiescent pool of liquid fuel, surface-tension-driven flow is initiated transiently. The ignition flame is supported by a controlled supply of propane through a capillary tube of i-d 3 mm. The resultant diffusion flame is about 2 cm long. The bottom part of this flame is nearly spherical in shape with a diameter of about 5 mm. It is this nearly spherical region which acts as the energy source for the liquid fuel, the separation distance between the bottom of the flame and the liquid surface being about 5 mm also. Typical liquid phase flow patterns are already presented in Plate II. For all fuel supply temperatures tested (in the range of about 28 ^{o}C - 36 ^{o}C) the ignition time is in the range of 0.1 to 1 second. In fact, this fractionally variant ignition time is difficult to be measured accurately. Consequently, we satisfied outselves with visual and photographic observations of the development of surface-tension flows.

Inasmuch as this compromise is made to limit our ignition experiments to observations of the liquid phase flow evolvement with time, we wondered if a heat source adjacent to a pool of water would produce a transient surface-convection-induced flow similar to that induced

in butanol. Our attempts failed to produce any distinct patterns but a similar unusual behavior of water has also been observed by other investigators such as MacDonald [4], and Berg [45]. The inevitable presence of impurities in water which would greatly influence the surface tension is claimed by these authors to be responsible for the observed anamoly between theoretical predictions and experimental observations.

7. Conclusions: These experiments lead to the conclusions which are listed in the main body of the report (Chapter V).

REFERENCES

1. Kanury, A. M., "Burning of Liquid Pools in Reduced Gravity," Final Report. NASA Contract NAS3-20087, University of Notre Dame, Notre Dame, Indiana, (June 1977).

2. Glassman, I., Sirignano, W. A., and Summerfield, M., "Physics of Flames," Final Report, U. S. Army Ballistic Research Laboratories Contract No. DAA 05-68-C-0450, Princeton University, Princeton, N.J. (1970).

3. Murad, R. J., Lamendola, J., Isoda, H., and Summerfield, M., "A Study of Some Factors Influencing the Ignition of a Liquid Fuel Pool," Combustion and Flame, pp. 289-298, 15, (1970).

4. MacDonald, B. W., "Preignition Motion of Liquid Fuels Due to Local Heat Input at the Upper Surface," M.S. Thesis in Engineering, Princeton University, (1972).

5. Glassman, I., and Hansel, J. G., "Some Thoughts and Experiments on Liquid Fuel Spreading, Steady Burning and Ignitability in Quiescent Atmospheres," Fire Res. Abs. and Revs., 10, No. 3, pp. 217-234 (1968).

6. MacKinven, R., Hansel, J. G., and Glassman, I., "Influence of Laboratory Parameters on Flame Spread Across Liquid Fuels," Comb. Sci. and Tech., 1, pp. 293-306 (1970).

7. Sirignano, W. A., and Glassman, I., "Flame Spreading Above Liquid Fuels: Surface-Tension-Driven Flows," Comb.Sci. and Tech., 1, pp. 307-312 (1970).

8. Torrance, K. E., "Subsurface Flows Preceding Flame Spread Over a Liquid Fuel," Comb.Sci. and Tech., 3, pp. 113-143 (1971).

9. Torrance, K.E., and Mahajan, R. L., "Surface Tension Flows Induced by a Moving Thermal Source," Comb. Sci. and Tech., 10, pp. 125-136 (1975).

10. Roberts, A. F., "Spread of Flame on a Liquid Surface," Ph.D. Thesis, Imperial College, London (1959).

11. Burgoyne, J. H., Roberts, A. F., and Quinton, P. G., "The Spread of Flame Across a Liquid Surface, I. The Induction Period; II Steady State Conditions; III. A Theoretical Model," Proc. Royal Soc. A.308, p. 39, 55 and 69 (1968).

12. Labus, T. L., Unpublished Work, NASA Lewis Research Center, Cleveland, Ohio (1978).

13. Kanury, A. M., "Methods of Measurements in Destructive Fires," pp. 279-296 in Experimental Diagnostics in Combustion of Solids, vol. 63 of Progress in Astronautics and Aeronautics, T. L. Boggs and B. T. Zinn, Editors. American Institute of Aeronautics and Astronautics, New York, N.Y. (1978).

14. McAdams, W. H., Heat Transmission, McGraw-Hill Book Co., New York (1954).

15. Blackshear, P. L. Jr., and Kanury, A. M., "Some Effects of Size, Orientation, and Fuel Molecular Weight on the Burning Rate of Fuel-Soaked Wicks," Eleventh Symposium (International) on Combustion, the Combustion Institute, Pittsburgh, pp. 545-552 (1967).

16. Blackshear, P. L. Jr., and Kanury, A. M., "Heat and Mass Transfer To, From and Within Cellulosic Solids Burning in Air," Tenth Symposium (International) On Combustion, The Combustion Institute, Pittsburgh, PA., pp. 911-923 (1965).

17. Reynolds, W. C., and Satterlee, H. M., "Liquid Propellant Behavior at Low and Zero g," Chapter 11 in The Dynamic Behavior of Liquids in Moving Containers, Edited by P. B. Abramson, NASA SP-106, National Aeronautics and Space Administration, Washington, D.C. (1967).

18. Reynolds, W. C., Saad, M. A. and Satterlee, H. M., "Capillary Hydrostatics and Hydrodynamics at Low-g," Tech. Rept. No. LG-3, Dept. of Mechanical Engineering, Stanford University, (1964).

19. Saunders, O. A.,"The effect of Pressure Upon Natural Convection in Air," Proceedings of Royal Society, A157, London,pp. 278-291 (1936).

20. Williams, F. A.,"Scaling Mass Fires," Fire Research Abstracts and Reviews, 11, (1), pp. 1-22, (1969).

21. de Ris, J., Kanury, A. M., and Yuen, M. C., "Pressure Modeling of Fires," pp. 1033-1044, Fourteenth Symposium (International) on Combustion, the Combustion Institute, Pittsburgh, PA (1973).

22. Kanury, A. M., "Modeling of Pool Fires with a Variety of Polymers," Fifteenth Symposium (International) on Combustion, The Combustion Institute, Pittsburgh, PA, pp. 193-202, (1975).

23. Baker, D. J., "A Technique for Precise Measurement of Small Fluid Velocities," Journal of Fluid Mechanics, 26, pp. 573-575,(1966).

24. Husar, R. B. and Sparrow, E. M., "Patterns of Free Convection Flow Adjacent to Horizontal Heated Surfaces," International Journal of Heat and Mass Transfer, 11, pp. 1206-1208 (1968).

25. Lloyd, J. R., and Sparrow, E. M., "On the Stability of Natural Convection Flow on Inclined Plates," J. Fluid Mech. 42, part 3, pp. 465-470, (1970).

26. Kumagai, S., "Combustion of Fuel Droplets in a Falling Chamber with Special Reference to the Effect of Natural Convection," Jet Propulsion, 26, p. 786, (1956).

27. Kumagai, S., and Isoda, H. "Combustion of Fuel Droplets in a Falling Chamber," Sixth Symposium (International) on Combustion, Reinhold Pub. Co., New York, pp. 726-731 (1957).

28. Isoda, H., and Kumagai, S., "New Aspects of Droplet Combustion," Seventh Symposium (International) on Combustion, Butterworths, London, pp. 523-531, (1959).

29. Edelman, R. B., Fortune, O. F., Weilerstein, G., Cochran, T. H., and Haggard, J. B. Jr., "An Analytical and Experimental Investigation of Gravity Effects Upon Laminar Gas Jet Diffusion Flames," Fourteenth Symposium (International) on Combustion, The Combustion Institute, Pittsburgh, PA., pp. 399-412, (1973).

30. Cochran, T. H., and Masica, W. J., "An Investigation of Gravity Effects on Laminar Gas Jet Diffusion Flames," Thirteenth Symposium (International) on Combustion, The Combustion Institute, Pittsburgh, PA, pp. 821-829, (1970).

31. Cochran, T. H., "Experimental Investigation of Laminar Gas Jet Diffusion Flames in Zero Gravity," NASA TN D-6523, (1972).

32. Haggard, J. B., and Cochran, T. H., "Stable Hydrocarbon Flames in a Weightless Environment," Combustion Science and Technology, 5, pp. 291-298, (1972).

33. Cochran, T. H., and Masica, W. J., "Effects of Gravity on Laminar Gas Jet Diffusion Flames," NASA TN-5872, (1970).

34. Haggard, J. B., and Cochran, T. H., "Hydrogen and Hydrocarbon Diffusion Flames in a Weightless Environment," NASA TN D-7165, (1973).

35. Kimzey, J. H., "Flammability in Zero Gravity," 55th AIChE National Meeting, Feb. 7-11, 1965, Houston, Texas, (1965).

36. Kimzey, J. H., "Flammability During Weightlessness," NASA TMX-58001, (1966).

37. Kimzey, J. H., Downs, W. R., Eldred, C. H., and Norris, C. W., "Flammability in Zero-Gravity Environment," NASA TR R246, (1966).

38. Kimzey, J. H., "Zero Gravity Flammability," in ME 69-1, GC Marshall Space Flight Center Mtg. Space Processing and Manufacturing, Oct. 21-22, 1969, Huntsville, Ala., (1969).

39. Pearce, J. P., Kimzey, J. H., and Pippen, D. L., "Effects of Gravity on Flammability," pp. 137-139 in NASA SP-5096, Conference on Materials for Improved Fire Safety, MSC, Houston, TX, (1970).

40. Levich, V. G., Physicochemical Hydrodynamics, Prentice-Hall, Inc., Englewood Cliffs, N.J. (1962).

41. Yih, C. S., "Fluid Motion Induced by Surface-Tension Variation," Physics of Fluids, 11, pp. 477-480 (1968).

42. Adler, J., "Fluid Mechanics of a Shallow Fuel Layer Near a Burning Wick," Comb. Sci. and Tech., 2, pp. 105-113, (1970).

43. Goldstein, S., Modern Developments in Fluid Dynamics, Dover Publications, New York, N.Y. (1965).

44. Merzkirch, W., Flow Visualization, Academic Press, New York, N.Y., (1974).

45. Berg, J. C., Boudart, M., and Acrivos, A., "Natural Convection in Pools of Evaporating Liquids," Journal of Fluid Mechanics, 24, (4), pp. 721-735, (1966).

46. Landau, L. D., and Lifschitz, E. M. Fluid Mechanics, pp. 241 et seq. Pergamon Press, (1959).

47. Birikh, R. V., "Thermocapillary Convection in a Horizontal Layer of Liquid," Journal of Applied Mechanics and Technical Physics, 7, No. 3, pp. 43-44, (1966).